

25-1 200

AD 646133

A Theoretical Estimate of Turbulent Wall Pressure Fluctuations on a Compliant Boundary

FRANK M. WHITE
ROBERT E. QUAGLIERI



DDP
RECEIVED
FEB 3 1967
B.

23 November 1966

Distribution of this document is unlimited.

U. S. Navy Underwater Sound Laboratory
Fort Trumbull, New London, Connecticut

ARCHIVE COPY

7	DISC.	AVAIL. AND/OR SPECIAL
	BY SECTION/AVAILABILITY CODES	
	CLASSIFICATION	
	BY APPROVED	
	WHITE SECTION	
	ORF SECTION	

ABSTRACT

A theoretical estimate is attempted for the effect of a compliant coating on turbulent boundary layer wall pressure fluctuations. The basic derivation shows that the problem reduces to one of finding the distribution in the wall plane of two correlations involving the wall pressure and its normal derivative. Exact expressions are derived for two-dimensional traveling wave pressure/velocity admittances of an isotropic elastic coating. These admittances are combined with some reasonable assumptions about the form of the pressure cross spectral density to yield approximate expressions for the two desired pressure/derivative correlations. Finally, two surface integrals of these correlations result in the wall pressure function in the presence of the compliant boundary. The calculations indicate that the compliant wall increases the mean square wall pressure at low speeds and decreases the pressure fluctuations at high speeds. Unfortunately, the reduction at high speeds probably cannot be achieved in practice because of the related mechanical problem of static divergence of the coating.

ADMINISTRATIVE INFORMATION

This report is the result of a study performed for the Laboratory by the authors under contract NPS UNWATSNLAB-2 and -3 and Contract No. 70024-44754. Dr. White is an Associate Professor of Mechanical Engineering at the University of Rhode Island, and Mr. Quaglieri was a graduate student at the time the report was prepared. The Laboratory project number is 1-509-00-00, and the corresponding Navy subproject and task number is SF 113 11 08-1356.

REVIEWED AND APPROVED: 23 November 1966

H. E. Nash
H. E. Nash
Technical Director

R. L. Corkran, Jr.
R. L. Corkran, Jr., Captain, USN
Commanding Officer and Director

TABLE OF CONTENTS

	Page
LIST OF ILLUSTRATIONS	iii
LIST OF TABLES	iv
INTRODUCTION	1
BASIC ANALYSIS	2
TRAVELING WAVE ADMITTANCES	5
Admittance Solution for Plane Strain	11
PRESSURE DERIVATIVE CORRELATIONS AT THE COMPLIANT WALL	13
NUMERICAL EVALUATION OF COMPLIANT COATING INTEGRALS	18
PRESSURE ATTENUATION BENEATH A COMPLIANT COATING	22
LIST OF REFERENCES	25
INITIAL DISTRIBUTION LIST	Inside Back Cover

LIST OF ILLUSTRATIONS

Figure		Page
1	Schematic of the Flow Geometry	27
2	Comparison of Normal Admittance Y_n for the Bonded and Shearless Coating	28
3	Comparison of Tangential Admittance Y_t and Normal Admittance Y_n for a Shearless Coating	29
4	Magnitude of the Asymptotic Plane Stress Admittances as a Function of Speed Ratio	30
5	Comparison of the Normal Admittance Y_n for Plane Stress versus Plane Strain	31
6	Comparison of Exact and Approximate Normal Admittances Y_n for Plane Strain	32
7	Experimental Data for the Power Spectrum of Rigid Wall Turbulent Pressure	33
8	Illustration of the Effect of Thickness Ratio (h/δ) on the Integrand of Eq. (40)	34
9	Normalized Distribution of the Correlation $\overline{P^* \frac{\partial P^{**'}}{\partial y^{**'}}}$	35
10	Normalized Distribution of the Correlation $\overline{\frac{\partial P^*}{\partial y^*} \frac{\partial P^{**'}}{\partial y^{**'}}}$	36
11	Final Estimation of the Effect of a Compliant Coating on the Wall Pressure	37
12	Effect of Coating Thickness on the Attenuation Constants in Eq. (52)	38
13	Pressure Attenuation Factor F as a Function of Frequency and Speed	39
14	Reduction of Undersurface Pressure Level as a Function of Speed Ratio and Thickness Ratio	40

LIST OF TABLES

Table		Page
1	Minimum Speed Ratio for an Admittance Singularity to Occur	10
2	Asymptotic Normal Admittances $(\rho_s C_s Y_n(\infty)/i)$ for $\mu = 0.5$	12
3	Normalized Excess Autocorrelation for a Thick Coating	21

A THEORETICAL ESTIMATE OF TURBULENT WALL PRESSURE FLUCTUATIONS ON A COMPLIANT BOUNDARY

INTRODUCTION

The problem of boundary layer behavior in the presence of a compliant boundary was brought to attention by the intriguing experiments of M. O. Kramer,^{1, 2, 3} who demonstrated reduced drag on underwater towed bodies covered by flexible coatings. Kramer intuitively ascribed the drag reduction to a transition delay provided by the dissipation of the compliant boundary. Subsequent theoretical studies, using an extension of the Orr-Sommerfeld stability equation, verified the transition delay but indicated that the cause was not added dissipation but rather a profound modification of the disturbance-wave structure of the flow. These linearized laminar stability studies were begun by Boggs and Tokita⁴ and later improved and extended by Benjamin,^{5, 6} Nonweiler,⁷ Linebarger,⁸ Landahl,⁹ Hains,¹⁰ and Kaplan.¹¹ Kaplan's thesis summarizes the previous work and contains extensive numerical stability calculations for a variety of model compliant boundaries.

Although the linearized theories definitely predict transition delay, the experiments which have followed Kramer's pioneering work have met only mixed success. The measurements of VonWinkle,¹² Boggs and Frey,¹³ and Laufer and Maestrello¹⁴ do not yield a definitive interpretation, largely because the transition delay, if it exists, is difficult to separate from whatever effect the coating might have on the fully turbulent region. It is hoped that measurements in the new water tunnel at the Underwater Sound Laboratory might clarify the matter.

The fully turbulent boundary layer in the presence of a compliant surface presents a formidable theoretical challenge. The sound radiated by turbulence near a flexible boundary has been estimated by Ffowcs Williams and Lyon,¹⁵ and the Reynolds stress very near the surface has been studied by Ffowcs Williams.¹⁶ To the authors' knowledge, there has been no theoretical study of turbulent wall pressure fluctuations at a compliant boundary, and it is the intent of the present report to present such a theory. The general development herein can easily be sifted for qualitative information. However, to produce quantitative results, the analysis has resorted to a series of approximations which probably reduce the final calculations to the status of a fairly crude estimate.

BASIC ANALYSIS

The basic problem of turbulent, boundary layer, wall pressure fluctuations has been the subject of intense experimental study over the past decade for the particular case of a rigid wall. Corcos¹⁷ gives an excellent review of the many published measurements of fluctuating pressure on a rigid wall. Probably the most accurate of these measurements are those of Bakewell et al.¹⁸ and Willmarth and Wooldridge,¹⁹ and it will be necessary to use these data in the analysis which follows. To the authors' knowledge, no measurements of fluctuating pressure at a compliant wall have appeared in the open literature.

Although measurements abound, theoretical work on turbulent wall pressure is lacking. Based on an approach suggested by Gardner,^{20, 21} a complete, though rather approximate, theory of the space-time distribution of rigid wall pressure has been given by White.²² White's analysis indicates that the statistical properties of pressure at a rigid wall are primarily affected by the shape of the mean velocity profile in the boundary layer. In particular, White's results predict that the longitudinal space correlation is affected significantly by the mean velocity profile, while the lateral correlation, the power spectrum, and the convection speeds are affected very little. Actual measurements seem insensitive to profile shape, a phenomenon Corcos¹⁷ calls "space-time similarity," although recent data by Schloemer²³ for pressure gradients indicate some profile effect, particularly on the power spectrum. This apparent overall insensitivity of rigid wall data is exploited in the present analysis.

The fluctuating pressure p may be calculated in principle for incompressible flow of a Newtonian fluid by taking the divergence of the Navier-Stokes equations, yielding the Poisson equation

$$\nabla^2 p = -\rho S(\tilde{X}, t) \quad (1)$$

where the function S is a complicated combination of velocity derivatives and t is time. The actual form of S is given by White²² and is not important in the present study. The position vector \tilde{X} has coordinates (x_1, x_2, x_3) which are sketched in Fig. 1. The freestream flows in the x_1 direction.

The formal solution of Eq. (1) for pressure at the wall ($x_2 = 0$) is given by Green's function integral solution:

$$\begin{aligned}
p(\tilde{X}, t) \Big|_{x_2=0} &= \frac{\rho}{2\pi} \int_0^{\infty} dz_2 \int_{-\infty}^{+\infty} dz_1 dz_3 \frac{S(\tilde{Z}, t)}{|\tilde{X} - \tilde{Z}|} \\
&- \frac{1}{2\pi} \int_{-\infty}^{+\infty} dz_1 dz_3 \frac{\left(\frac{\partial p}{\partial z_2}\right)_{z_2=0}}{|\tilde{X} - \tilde{Z}|}.
\end{aligned}
\tag{2}$$

Note that the second integral in Eq. (2) requires knowledge of a boundary condition in the form of the normal derivative of p at the wall. For a rigid wall, this derivative is negligibly small, by analogy with boundary layer theory, as Kraichnan²⁴ has shown. Thus, the rigid wall pressure is given simply by the first integral, which involves only the source term S . If we accept the experimental evidence that the wall-pressure correlation is insensitive to the form of S , then the effect of a compliant wall must be primarily due to changes in the boundary condition on p . It is the purpose of this report to investigate how the compliant surface might affect the normal derivative of p at the wall, so that the mean value of the second integral in Eq. (2) might be evaluated, at least approximately.

To shorten the expressions which follow, let P denote wall pressure p_w and let us rewrite Eq. (2) with the following tighter notation for the double and triple integrals:

$$P + \frac{1}{2\pi} \int_{x_2=0} \left(\frac{\partial P}{\partial z_2}\right) \frac{dZ}{|\tilde{X} - \tilde{Z}|} = \frac{\rho}{2\pi} \int_{x_2 > 0} \frac{S dZ}{|\tilde{X} - \tilde{Z}|}
\tag{3}$$

If we define the wall-pressure, space-time correlation by the relation

$$\overline{R(\tilde{X}, \tilde{X}', t, t')} = \overline{P(\tilde{X}, t) P(\tilde{X}', t')},
\tag{4}$$

where the overbar denotes the time average in the statistically stationary sense, then, by substituting into Eq. (3) and performing the time average underneath the integral signs, we obtain

$$\begin{aligned}
R + \frac{1}{2\pi} \int \frac{\overline{P \frac{\partial P'}{\partial z'_2}}}{|\tilde{X}' - \tilde{Z}'|} dZ' + \frac{1}{2\pi} \int \frac{\overline{P' \frac{\partial P}{\partial z_2}}}{|\tilde{X} - \tilde{Z}|} dZ + \\
+ \frac{1}{4\pi^2} \int \int \frac{\overline{\frac{\partial P}{\partial z_2} \frac{\partial P'}{\partial z'_2}}}{|\tilde{X} - \tilde{Z}| |\tilde{X}' - \tilde{Z}'|} dZ dZ' = \frac{\rho^2}{4\pi^2} \int \int \frac{\overline{S S'}}{|\tilde{X} - \tilde{Z}| |\tilde{X}' - \tilde{Z}'|} dZ dZ',
\end{aligned} \tag{5}$$

where the integrals involving P are to be evaluated in the planes ($z_2, z_2' = 0$) and the integrals involving S are evaluated in the infinite half space above this plane of the wall. After inspection, we find that the first two integrals on the left-hand side are identical because of symmetry in a plane.

It should be noted that the right-hand side involves the source terms S which occur in the boundary layer flow past whatever type boundary is under study. That is, if we seek to use Eq. (5) to calculate R for a compliant surface, then S should be the source function for flow past a compliant surface. It is at this point that we use the experimental insensitivity of the source function, previously discussed, to postulate that the right-hand side of Eq. (5) is essentially identical to R_0 , the pressure correlation in the presence of a rigid wall. This assumption, although reasonable, cannot be verified until data are available for mean and fluctuating velocities in the boundary layer past a compliant surface. Apparently Professor J. Lumley at the Pennsylvania State University is presently making such measurements. The question is also being examined theoretically at present by the second author as a thesis for the University of Rhode Island.

Combining the first two integrals in Eq. (5) and utilizing the assumption that the source integral is equal to R_0 , one obtains the following basic relation for calculating the wall pressure at a compliant surface:

$$R = R_0 - \frac{1}{\pi} \int \frac{\overline{P \frac{\partial P'}{\partial z'_2}}}{|\tilde{X}' - \tilde{Z}'|} dZ' - \frac{1}{4\pi^2} \int \int \frac{\overline{\frac{\partial P}{\partial z_2} \frac{\partial P'}{\partial z'_2}}}{|\tilde{X} - \tilde{Z}| |\tilde{X}' - \tilde{Z}'|} dZ dZ' \tag{6}$$

At first glance, Eq. (6) might appear to predict that the compliant wall correlation R is always less than the rigid wall value R_0 . However, we shall see that the first integral is usually negative, while the second integral is positive, with the result that the effect on R is rather mixed.

TRAVELING WAVE ADMITTANCES

Since R_0 is known from experiment, the evaluation of R from Eq. (6) can be accomplished if the correlations involving P and its normal derivative can be estimated. To do this, we must investigate the properties of an idealized elastic coating. All available experiments indicate that turbulent boundary layer fluctuating pressures have approximately the form of traveling waves moving in the x_1 direction with a convection velocity U_c somewhat less than the freestream velocity U_∞ . Naturally, there is a certain amount of convective incoherence, since the pressure waves as they move downstream are undergoing continuous decay and regeneration. No attempt will be made here to reproduce this effect; that is, the fluctuating pressures will be treated as a simple summation of traveling waves of different frequencies. A second difficulty is that the actual turbulent pressures are not plane waves but instead have some unknown variable shape in the lateral (x_3) direction. This analysis will treat the case of plane waves and then attempt belatedly to introduce a three-dimensional effect by use of the measured lateral spectra of wall pressure.

Consider a compliant coating of thickness h , backed up by a rigid under-surface, as shown in Fig. 1. Several studies have been made of the response of such a coating to a plane traveling wave for a Hookean isotropic coating, assuming small strains. The analytical results are in the form of traveling wave admittances, which are amplitude ratios of coating velocity to traveling wave pressure. Following a suggestion of Nonweiler,⁷ Kaplan¹¹ calculated admittances by assuming a condition of plane stress in the coating, while Tokita and Boggs²⁵ gave admittances for the case of plane strain. Both Kaplan's results and those of Tokita and Boggs contain algebraic errors which, hopefully, have been eliminated in the present report. Also, Tokita and Boggs, by expanding in a series and truncating, gave approximate admittances (equation 7b9 of Ref. 25) which they later used in a study of coating stability.²⁶ However, numerical evaluation of exact admittance formulas shows that these approximations are valid only for a small range of frequencies and hence will not be used here.

As is usual in elasticity theories, there is no great difference between the plane stress admittances and the plane strain results. Let us reproduce a plane stress analysis, similar to that of Kaplan,¹¹ comparing the final results obtained with those of Tokita and Boggs²⁵ for plane strain.

From Fig. 1, a streamwise plane traveling pressure wave would have the following complex form for any given frequency ω :

$$p = p_0 e^{i\omega\left(\frac{x_1}{U_c} - t\right)} = p_0 e^{i\alpha(x_1 - U_c t)}, \quad (7)$$

where U_c is the convection speed and $\alpha = \omega/U_c$ is the wave number. Let ξ be the coating displacement in the x_1 direction and η be the displacement in the x_2 direction. Let the elastic coating have shear modulus G , Poisson's ratio μ , and Young's modulus $E = 2G(1 + \mu)$. Then the equations of elasticity for plane stress are

$$\begin{aligned} \rho_s \frac{\partial^2 \xi}{\partial t^2} &= \frac{\partial \sigma_{11}}{\partial x_1} + \frac{\partial \sigma_{12}}{\partial x_2} \\ \rho_s \frac{\partial^2 \eta}{\partial t^2} &= \frac{\partial \sigma_{12}}{\partial x_1} + \frac{\partial \sigma_{22}}{\partial x_2} \\ \epsilon_{11} &= \frac{\partial \xi}{\partial x_1}; \quad \epsilon_{22} = \frac{\partial \eta}{\partial x_2}; \quad \epsilon_{12} = \frac{\partial \eta}{\partial x_1} + \frac{\partial \xi}{\partial x_2} \end{aligned} \quad (8)$$

$$E\epsilon_{11} = \sigma_{11} - \mu\sigma_{22}$$

$$E\epsilon_{22} = \sigma_{22} - \mu\sigma_{11}$$

$$G\epsilon_{12} = \sigma_{12}$$

Equation (8) contains eight linear algebraic and differential equations in the eight variables σ_{11} , σ_{22} , σ_{12} , ϵ_{11} , ϵ_{22} , ϵ_{12} , η , and ξ . The stresses and strains may easily be eliminated in favor of the two displacements for which boundary conditions are known at the upper and lower surface of the coating. Since the system is linear and the driving force is a traveling wave (Eq. (7)), it follows that the resulting displacements must also be traveling waves with amplitudes which vary through the thickness. Hence we postulate that

$$\begin{aligned} \xi(x_1, x_2, t) &= \xi_0(x_2) e^{i\alpha(x_1 - U_c t)} \\ \eta(x_1, x_2, t) &= \eta_0(x_2) e^{i\alpha(x_1 - U_c t)}. \end{aligned} \quad (9)$$

The exponential expressions will cancel properly from the equations of motion, leaving a single ordinary fourth order linear differential equation in $\eta_0(x_2)$:

$$\eta_0'''' - a^2(r_1^2 + r_2^2)\eta_0'' + a^4 r_1^2 r_2^2 \eta_0 = 0, \quad (10)$$

where the constants r_1 and r_2 are related to the ratio of the convection speed U_c to the coating shear wave speed $C_s = \sqrt{G/\rho_s}$, as follows:

$$\begin{aligned} r_1^2 &= 1 - \frac{1}{2} (1 - \mu) U_c^2 / C_s^2 \\ r_2^2 &= 1 - U_c^2 / C_s^2. \end{aligned} \quad (11)$$

The primes in Eq. (10) indicate differentiation with respect to x_2 . An equation identical to Eq. (10) holds for the other displacement, ξ_o .

The general solution of Eq. (10) is

$$\eta_o = A_1 \sinh(ar_1 x_2) + A_2 \cosh(ar_1 x_2) + A_3 \sinh(ar_2 x_2) + A_4 \cosh(ar_2 x_2), \quad (12)$$

where A_1 --- A_4 are constants. Assuming that the coating is securely bonded to the rigid understructure, the boundary conditions at the lower surface state that the displacements must vanish:

$$\xi_o(-h) = \eta_o(-h) = 0. \quad (13)$$

At the upper surface, the vertical normal stress in the coating must equal the traveling wave pressure:

$$\sigma_{22}(0) = \frac{2G}{1-\mu} \left[\frac{\partial \eta}{\partial x_2} + \mu \frac{\partial \xi}{\partial x_1} \right]_{x_2=0} = -p. \quad (14)$$

A simple and realistic fourth boundary condition is achieved by setting the shear stress equal to zero at the upper surface:

$$\frac{\partial \xi}{\partial x_2} + \frac{\partial \eta}{\partial x_1} = 0 \text{ at } x_2 = 0. \quad (15)$$

Actually, the shear stress at the upper surface does not vanish but instead must equal the fluid shear stress in the boundary layer at the wall, τ_w . However, τ_w is small, and the fraction of τ_w assigned to any given traveling wave

must be very small indeed. Hence this refinement is not considered to be necessary for an accurate calculation of the admittance of the coating.

Equations (13), (14), and (15) are sufficient to define unique values of the four constants A_i in Eq. (12). Since we will ultimately be concerned with velocities at the upper surface, it is convenient to give the solutions in terms of the admittances Y_n and Y_t , defined as follows:

$$\begin{aligned} Y_n &= -\frac{1}{\rho} \left(\frac{\partial \eta}{\partial t} \right)_{x_2=0} \\ Y_t &= +\frac{1}{\rho} \left(\frac{\partial \xi}{\partial t} \right)_{x_2=0} \end{aligned} \quad (16)$$

The negative sign in the definition of Y_n is traditional. Unfortunately, the admittances, although defined as ratios, are not dimensionless. It will be convenient to use the dimensionless group $(\rho_s C_s Y)$, which is a function of the dimensionless parameters r_1 , r_2 , and (ah) . The normal admittance is given by the expression

$$\rho_s C_s Y_n = \frac{-i r_1 (U_s/C_s)^3}{2(1+r_2^2)A_1 + 4r_1 r_2 A_3} \quad (17)$$

The constants A_2 and A_4 have been incorporated into Eq. (17), but the expressions for A_1 and A_3 are rather lengthy. If we adopt the short notation

$$\begin{aligned} C_i &= \cosh(ar_i h) \\ T_i &= \tanh(ar_i h) \end{aligned} \quad \text{for } i = 1, 2, \quad (18)$$

then A_1 and A_3 may be written as follows:

$$\begin{aligned} A_3 &= \frac{1 - r_1 r_2 T_1 T_2 - \frac{1}{2}(1+r_2^2)(1-T_1^2)C_1/C_2}{T_2 - r_1 r_2 T_1} \\ A_1 &= \frac{(1 - A_3 T_2)C_2/C_1 - \frac{1}{2}(1+r_2^2)}{T_1} \end{aligned} \quad (19)$$

In the limit as (αh) approaches infinity, T_1 and T_2 approach unity. By inspection, we see that A_3 will approach unity and A_1 becomes $-\frac{1}{2}(1+r_2^2)$. From Eq. (17), the admittance will approach the limiting value

$$\rho_n C_n Y_n(\infty) = \frac{-i r_1 (U_c/C_n)^3}{4 r_1 r_2 - (1 + r_2^2)^2} \quad (20)$$

The denominator of Eq. (20) becomes zero, giving infinite Y_n , at a speed ratio (U_c/C_n) varying from 0.874 for $\mu = 0$ to a value of 0.933 for $\mu = 0.5$. For speeds less than this critical value, the denominator is positive, and Eq. (17) predicts in general that Y_n will be a pure negative imaginary quantity for any subcritical speed.

Equation (17) applies for a coating which is perfectly bonded to the undersurface, i.e., it satisfies Eq. (13). If one relaxes this condition, a much simpler expression for Y_n results, as shown by Kaplan.¹¹ Instead of being bonded, we could postulate that the coating slides without shear along the lower surface, satisfying the following conditions:

$$\tau_1(-h) = \frac{\partial \xi}{\partial x_2}(-h) = 0 \quad (21)$$

The use of Eq. (21) instead of Eq. (13) gives a much simpler normal admittance, which we term the "shearless" coating result:

$$\rho_n C_n Y_n(\text{shearless}) = \frac{-i r_1 (U_c/C_n)^3}{4 r_1 r_2/T_2 - (1 + r_2^2)^2/T_1} \quad (22)$$

Clearly, the limit of Eq. (22) as (αh) approaches infinity is identical to Eq. (20) for the bonded coating. In general, for a given subcritical speed, there is no great difference between the bonded and the shearless coating over the entire frequency range, as Fig. 2 shows, using $\mu = 0.5$ as an approximate value for natural rubber. As Fig. 2 indicates, the shearless admittances at low frequencies are about twenty per cent higher than the bonded values. The high frequency asymptotes are identical.

The tangential admittance Y_t as defined in Eq. (16) may also be calculated. The result for the bonded coating is

$$\rho_s C_s Y_t = \frac{-(U_c/C_s) (r_1 r_2 A_3 + A_1)}{2 r_1 r_2 A_3 + A_1 (1 + r_2^2)}, \quad (23)$$

where A_1 and A_3 are again defined by Eq. (19). Once again a simpler expression results for the "shearless" coating:

$$\rho_s C_s Y_t (\text{shearless}) = \frac{-(U_c/C_s) (2 r_1 r_2 - (1 + r_2^2) T_2/T_1)}{4 r_1 r_2 - (1 + r_2^2)^2 T_2/T_1}. \quad (24)$$

As before, the admittance is slightly larger for the shearless coating as compared to the bonded value. Figure 3 compares the tangential and normal admittances for the shearless coating for $\mu = 0.5$. The asymptotic values of Y_t are roughly one-half of the asymptotic magnitude of Y_n for the same speed ratio. The tangential admittance suffers a singularity at the same "critical" speed ratio as Y_n , as listed in Table 1.

Table 1

MINIMUM SPEED RATIO FOR AN ADMITTANCE SINGULARITY TO OCCUR

Poisson's Ratio	Minimum (U_c/C_s)
0.0	0.8740
0.1	0.8913
0.2	0.9052
0.3	0.9162
0.4	0.9252
0.5	0.9325

As we shall see in the next section, the evaluation of Eq. (6) for a reasonably thick coating (of the order of the boundary layer thickness) depends only upon the asymptotic values of Y_n . Figure 4 shows the magnitude of these asymptotic admittances for subcritical speeds. Note that, for low speeds, the asymptotic admittances vary linearly with speed ratio.

ADMITTANCE SOLUTION FOR PLANE STRAIN

The previous theoretical admittances, Eqs. (17) through (24), are derived for the assumption of plane stress (zero stress in the z direction). The analogous solution for plane strain (zero z displacement) was given by Tokita and Beggs,²⁵ following a somewhat more complicated analysis, using the three-dimensional wave equation which results from the definition of the so-called "displacement potentials." The boundary conditions used were Eqs. (13) and (15), that is, a tightly bonded coating. An exact expression for the admittance was not given but can easily be calculated from equation (7b6) of Ref. 25. The parameter r_2 is the same as for plane stress, but the quantity r_1 is slightly different. That is,

$$r_2^* = 1 - U_c^2/C_s^2$$

$$r_1^{*2} = 1 - \frac{1}{2} \frac{(1 - 2\mu)}{(1 - \mu)} U_c^2/C_s^2, \quad (25)$$

where the asterisk is included in r_1^* as a reminder that it is the plane strain value. Using this notation, the exact expression for the normal admittance for plane strain in a bonded coating is

$$\rho_s C_s Y_n = \frac{-i r_1^* (U_c/C_s)^3 (T_1^* - r_1^* r_2 T_2)}{4 r_1^* r_2 (1 - r_1^* r_2 T_1^* T_2) - (1 + r_2^2)^2 (r_1^* r_2 - T_1^* T_2) - 4 r_1^* r_2 (1 + r_2^2)/C_1^* C_2}, \quad (26)$$

where T_i and C_i are as defined in Eqs. (18). Figure 5 compares values of Y_n from Eq. (26) to equivalent values for the plane stress case, Eq. (17). For a given speed ratio, the plane strain admittance is somewhat smaller and has a lower asymptote. The high frequency asymptote of Eq. (26) is

$$\rho_s C_s Y_n(\infty) = \frac{-i r_1^* (U_c/C_s)^3}{4 r_1^* r_2 - (1 + r_2^2)^2} \quad (27)$$

which is identical in form to Eq. (20) for the plane stress case. Table 2 gives a comparison of these asymptotic values.

Table 2
 ASYMPTOTIC NORMAL ADMITTANCES $(\rho_n C_n Y_n(\infty)/i)$ FOR $\mu = 0.5$

U_c/C_s	PLANE STRESS	PLANE STRAIN
0.2	- 0.1374	-0.1031
0.4	- 0.3038	-0.2282
0.6	- 0.5676	-0.4232
0.7	- 0.8118	-0.5950
0.8	- 1.3406	-0.9302
0.85	- 2.0189	-1.2926
0.9	- 4.6190	-2.2262
0.91	- 6.4855	-2.6433
0.92	-11.3029	-3.2873
0.93	-54.1007	-4.4247

Although the plane strain values in Table 2 are substantially smaller in magnitude, we shall see that this has no great effect on the wall pressure analysis which follows. However, since a practical coating construction would probably be constrained in a manner somewhere in between these two extremes, one can look upon Table 2 as a measure of the uncertainty involved in a theoretical estimate of the actual coating response to traveling waves.

As mentioned before, Ref. 25 did not attempt to calculate the exact plane strain admittance as given by Eq. (26). Instead, Tokita and Boggs approximated the hyperbolic functions by the first two terms of their Taylor series expansions. The result was an approximate admittance expression (equation (7b9) of their report). In the present notation, this approximation is written as

$$\rho_s C_s Y_n \doteq \frac{-2 \alpha^3 h^3}{3 (\alpha^2 h^2 - 2) (U_c^2/C_s^2 - k^2)}, \quad (28)$$

where

$$k^2 = \frac{4 \alpha^2 h^2}{\alpha^2 h^2 (3 - 4\mu) - 4 (1 - \mu)}$$

Figure 6 compares the exact admittance from Eq. (26) with the approximate value, Eq. (28), for the case $(U_c/C_s) = 0.5$ and $\mu = 0.5$. It is seen that Eq. (28) is accurate only for a small intermediate frequency range. Note that Eq. (28) fails to predict a constant asymptotic admittance at high frequencies. The approximate admittance, although apparently rather crude, was used by Tokita and Boggs in Ref. 26 to predict the mechanical stability (static divergence and flutter) of a compliant coating. Since their calculations were rather complex and also involved further approximations, it is not clear exactly what quantitative effect the error inherent in Eq. (28) would introduce into the results of Ref. 26.

Finally, we may note that, for "supercritical" speeds (greater than those in Table 1), all of the admittance expressions possess multiple singularities. Since Ref. 26 predicts a statically unstable coating at such speeds, no supercritical calculations were made in this report.

PRESSURE DERIVATIVE CORRELATIONS AT THE COMPLIANT WALL

The chief result of the basic analysis section of this report was to show that the problem of estimating compliant surface pressure fluctuations reduces approximately to the evaluation of Eq. (6). The first integral in Eq. (6) cannot be evaluated until we know the distribution of the correlation function $\overline{P(\partial P')/\partial x_2'}$ in the plane of the wall. The second integral requires knowledge of the correlation $\overline{(\partial P \partial P')/(\partial x_2 \partial x_2')}$ in the wall plane. It is the purpose of this section to show that these correlations can be reasonably approximated, using the traveling wave admittance approach.

It is obviously necessary to the admittance approach that we assume that the turbulent pressure disturbances are in the form of a superposition of many small traveling waves having different amplitudes and frequencies. This is certainly not true on an instantaneous basis. That is, turbulent pressure fluctuations suffer by nature a convective incoherence. The disturbances are constantly decaying and being regenerated as they move downstream with a constantly changing convection speed. It is only on a time-averaged basis that the

pressure simulates in any way a sum of traveling waves. Some evidence of convective incoherence persists even on a time-average basis. For example, the convection speed U_c is not truly constant but instead varies with the frequency and with the spacing between correlated points. Also, the sharp decrease in the pressure correlation with lateral spacing indicates that the assumption of plane traveling waves is not very accurate, even on the average. However, it is fortuitous that these deviations from ideal traveling wave behavior do not have a strong effect on the behavior of a compliant boundary, because, as the calculations will show, the compliant wall responds in an extremely localized fashion to the pressure disturbances. That is, the correlations needed in Eq. (6) drop off so rapidly with distance that their effect on the calculation of R in Eq. (6) is confined to a small local region whose diameter is less than a boundary layer thickness. Under these conditions, the convective incoherence, which occurs on a somewhat larger scale, does not cause any great error in the analysis.

The normal derivative of P is related to the velocity components through the normal component of the Navier-Stokes equations:

$$-\frac{1}{\rho} \frac{\partial P}{\partial x_2} = \frac{\partial u_2}{\partial t} + u_1 \frac{\partial u_2}{\partial x_1} + u_2 \frac{\partial u_2}{\partial x_2} - \mu \nabla^2 (u_2). \quad (29)$$

For a rigid wall, u_1 and u_2 both vanish at the wall, leaving only the viscous term on the right-hand side of Eq. (29). As mentioned before, Kraichnan²⁴ showed this viscous term to be negligibly small for a rigid wall. However, for a compliant wall, none of the velocity terms in Eq. (29) vanish, and care must be taken to ascertain their magnitude. The no-slip condition should still be valid, so that the fluid velocities at the wall must equal the surface velocities in the coating, which in turn are related through the admittance functions to the fluctuating wall pressure. The use of coating velocity instead of fluid velocity allows us to ignore the interplay between the fluid's mean and fluctuating velocities - an interplay which has caused erroneous results in stability studies, e.g., Ref. 4.

To evaluate the terms in Eq. (29), consider first a single traveling wave of amplitude P_0 . Using the admittance concept, one can calculate the amplitude of the normal acceleration at the coating surface:

$$\left| \frac{\partial u_2}{\partial t} \right| = \left| Y_n \right| \omega P_0. \quad (30)$$

In a similar manner we obtain an estimate of the first convective term in Eq. (29):

$$\left| u_1 \frac{\partial u_2}{\partial x_1} \right| \doteq \left| Y_n Y_t \right| \alpha P_o^2 . \quad (31)$$

Let us denote the dimensionless tangential admittance by the symbol $Y_t^* = \rho_s C_s Y_t$. Then the ratio of these two terms is, approximately:

$$\frac{\left| u_1 \frac{\partial u_2}{\partial x_1} \right|}{\left| \frac{\partial u_2}{\partial t} \right|} \doteq Y_t^* \frac{P_o}{\rho_s C_s U_c} . \quad (32)$$

From Fig. 4, Y_t^* is less than 5 for U_c/C_s less than 0.8, while the dimensionless pressure amplitude $P_o/(\rho_s C_s U_c)$ is much smaller than unity. Then, for a single traveling wave, the first convective term is negligibly small compared to the local normal acceleration. Then, by superimposing a large number of traveling waves, one arrives at the root-mean-square approximation:

$$\frac{\left(u_1 \frac{\partial u_2}{\partial x_1} \right)_{rms}}{\left(\frac{\partial u_2}{\partial t} \right)_{rms}} = \mathcal{O} \left(Y_t^* \frac{\bar{P}_{rms}}{\rho_s C_s U_c} \right) . \quad (33)$$

All available measurements indicate that the root-mean-square turbulent pressure $\bar{P}_{rms} \doteq 0.003 \rho U_\infty^2$, where ρ is the fluid density and U_∞ is the freestream velocity. Thus, the dimensionless pressure in Eq. (33) is a very small fraction for subcritical speeds, making the first convective term negligible. A similar comparison of the second convective term to the local acceleration yields exactly the same order of magnitude estimate as that of Eq. (33), so that this term is also quite small. Finally, the ratio of the viscous term in Eq. (29) to the local acceleration is found to be of order c_f , the local skin friction coefficient. Since c_f for a turbulent boundary layer is approximately 0.005 or less, the viscous term is also negligible. Clearly, then, the pressure normal derivative in Eq. (29) is dominated by the local normal acceleration, and an accurate estimate to the first of the two desired pressure correlations is:

$$\overline{P \frac{\partial P'}{\partial x_2'}} = -\rho \overline{P \frac{\partial u_2'}{\partial t'}} \quad (34)$$

To evaluate Eq. (34), we note that, for a single traveling wave, the correlation between P and the normal acceleration would be

$$P_o \left| \frac{\partial u_2}{\partial t} \right| = i Y_n \omega P_o^2 \quad (35)$$

To generalize this expression to a complete distribution of traveling waves, we make use of the space-frequency correlation Γ of the wall pressure, which is the Fourier transform of the space-time correlation R defined in Eq. (4);

$$R(\xi, \eta, t_o) = \int_{-\infty}^{\infty} \Gamma(\xi, \eta, \omega) e^{i t_o \omega} d\omega, \quad (36)$$

where ξ , η , and t_o are the longitudinal separation, the lateral separation, and the time delay between the two correlated boundary points, respectively. Utilizing this function Γ to generalize Eq. (35), we obtain the following expression for the first desired pressure correlation function:

$$\overline{P \frac{\partial P'}{\partial x_2'}} = -i \rho \int_{-\infty}^{\infty} \omega Y_n \Gamma e^{i t_o \omega} d\omega, \quad (37)$$

where Y_n is taken to be frequency dependent as given by Eq. (17), for example, for a bonded coating. Equation (37) is not an exact representation unless Y_n is given spatial properties to account for the fact that turbulent pressure disturbances are not purely plane waves. The authors have not attempted to introduce such a sophisticated admittance function into this analysis, arguing in the previous paragraphs that the "localized" behavior of the coating makes a spatially distributed admittance unnecessary.

Extensive measurements are available for the frequency correlation Γ_o for the case of a rigid wall. For zero separation, Γ_o reduces to the power spectrum $\phi_o = \Gamma_o(o, o, \omega)$. The data of Ref. 18 show that the dimensionless power spectrum $(\phi_o U_x / \delta \tau_r^2)$ is essentially a function of the Strouhal number $(\omega \delta / U_x)$, with negligible Reynolds number effect. Let ϕ^* and ω^* denote these two dimensionless variables. Figure 7 shows the data of Bakewell et al.,¹⁸ compared with the simple empirical formula

$$\phi^* = \frac{0.16}{1 + .012 \omega^{*2} + .0000036 \omega^{*4}} \quad (38)$$

Equation (38) is convenient for the calculations which follow. For example, the area under the ϕ^* curve equals the dimensionless mean square pressure, as Eq. (36) shows. Equation (38) may be integrated exactly to give the result $\overline{P_{rms}} = 2.0 \tau_w$, which is the commonly accepted experimental value without a transducer-size correction. Let us now define dimensionless variables:

$$\begin{aligned} P^* &= P/\tau_w \\ y^* &= x_2/\delta \\ \Gamma^* &= \Gamma U_x/(\delta \tau_w^2) \\ Y_n^* &= \rho_n C_n Y_n/i \\ t_0^* &= t_0 U_x/\delta \end{aligned} \quad (39)$$

In terms of these variables, Eq. (37) may be rewritten in dimensionless form:

$$\overline{P^* \frac{\partial P^{*'}}{\partial y^{*'}}} = \frac{\rho}{\rho_n} \frac{U_x}{C_n} \int_{-\infty}^{\infty} \omega^* Y_n^* \Gamma^* e^{i \omega^* t_0^*} d\omega^* \quad (40)$$

We note from the coefficient of the integral that the correlation must, for a given value of the ratio (h/δ) , be proportional to the fluid density and freestream velocity, i.e., the mass flow per unit area past the coating.

In an exactly similar manner, we arrive at a dimensionless expression for the second desired correlation function:

$$\overline{\frac{\partial P^*}{\partial y^*} \frac{\partial P^{*'}}{\partial y^{*'}}} = \left(\frac{\rho}{\rho_n} \frac{U_x}{C_n} \right)^2 \int_{-\infty}^{\infty} \omega^{*2} Y_n^{*2} \Gamma^* e^{i \omega^* t_0^*} d\omega^* , \quad (41)$$

indicating that this correlation is proportional to the square of the mass flow past the coating. As the next section shows, the integration is somewhat complicated by the fact that Y_n^* and Γ^* depend on system parameters other than simply the frequency ω^* .

NUMERICAL EVALUATION OF COMPLIANT COATING INTEGRALS

In carrying out the integrations given in Eqs. (40) and (41), we first note that the argument of Y_n^* is not simply ω^* but instead involves the coating thickness and the convection speed. That is,

$$Y_n^* = Y_n^* (\omega h/U_c) = Y_n^* [\omega^* (h/\delta) (U_\infty/U_c)]. \quad (42)$$

For a given Reynolds number and pressure gradient, the ratio (U_∞/U_c) is roughly constant, with a value varying from approximately 1.0 for a high Reynolds number and/or favorable pressure gradient to a value of about 2.0 for a low Reynolds number and/or adverse gradient. References 17, 18, 19, and 23 give measured values of this ratio for various flow conditions. For a given flow, then, Eq. (42) shows that the function Y_n^* shifts to the right along the ω^* axis as the thickness ratio (h/δ) decreases. This effect is sketched in Fig. 8, which compares Y_n^* for various thicknesses to the remainder of the integrand of Eq. (40). Since, as already noted, Y_n^* has an asymptotic constant value, the value of the integrand will approach a constant distribution no matter how much the coating thickness is increased. In practice, an increase of the coating thickness beyond $(h/\delta) = 1.0$ has little or no effect on the integration. Thus, according to the present analysis, a coating designed for noise attenuation need not be more than the thickness of the boundary layer itself.

The cross spectral density Γ varies considerably with the spacing coordinates ξ and η . For a rigid wall, Corcos²⁷ suggests the following empirical formula which approximates the existing data:

$$\Gamma_o^* = \phi_o^* \exp [- (\omega/U_c) (+ 0.11 \xi + 0.60 \eta + i \xi)], \quad (43)$$

where the subscript "o" indicates the rigid wall case. As a first approximation to the evaluation, we assume that the compliant surface spectrum Γ required in Eqs. (40) and (41) is identical to Eq. (43) except that the power spectrum ϕ^* has an adjustable magnitude:

$$\phi_{\text{coating}}^* = B / (1 + .012 \omega^{*2} + .0000036 \omega^{*4}), \quad (44)$$

where $B = 0.16$ for the rigid wall from Eq. (38). Although this seems to be a crude estimate a priori, the calculations which follow show it to be actually

quite accurate, so that a second approximation was not needed. Non-dimensionalizing the separations by the boundary layer thickness, we have the following reasonable formula:

$$\Gamma_{\text{coating}}^* = \phi_{\text{coating}}^* \exp[-\omega^* (U_x/U_c) (a \xi^* + b \eta^* + i \xi^*)], \quad (45)$$

where $a = 0.11$ and $b = 0.50$, approximately. Equation (40) becomes

$$\overline{P^* \frac{\partial P^{**'}}{\partial y^{**'}}} = 2 \frac{\rho U_x}{\rho_s C_s} \int_0^\infty \omega^* Y_n^* \phi^* e^{-\omega^* (U_x/U_c) (a \xi^* + b \eta^*)} \cos[\omega^* (t_0^* - (U_x/U_c) \xi^*)] d\omega^*. \quad (46)$$

The integration is laborious but easily accomplished on a digital computer. Note that the integral depends upon only two parameters, which are the coefficients of ω^* in the exponential and cosine terms, respectively. For a thick coating ($h \geq \delta$), Y_n^* may be taken equal to its asymptotic value. The maximum value of the integral clearly occurs for zero separation and zero time delay with a thick coating. This maximum may be calculated exactly if ϕ^* is assumed to follow Eq. (44). The result is

$$\overline{\left(\frac{\partial P^{**'}}{\partial y^{**'}} \right)_{\max}} = 319.4 (\rho U_x / \rho_s C_s) Y_n^*(\infty) B, \quad (47)$$

which may be used to normalize the integral in Eq. (46). Figure 9 shows the resulting normalized correlation as a function of its two parameters. This normalized space-time distribution is ready to be substituted into the first integral of Eq. (6) as a contribution to the compliant wall pressure correlation R .

In an exactly similar manner, Eq. (45) may be substituted into Eq. (41) to evaluate the second desired pressure-derivative correlation. The maximum value of this quantity again occurs at zero separation and time delay:

$$\overline{\left(\frac{\partial P^*}{\partial y^*} \frac{\partial P^{**'}}{\partial y^{**'}} \right)_{\max}} = 13175 [(\rho U_x / \rho_s C_s) Y_n^*(\infty)]^2 B. \quad (48)$$

Figure 10 shows the second desired correlation normalized by Eq. (48). This distribution is ready to be substituted into the second integral in Eq. (6).

The evaluation of the two integrals in Eq. (6) is a tedious but straightforward proposition. All such laborious computations in this report were performed on the IBM 1410 computer at the University of Rhode Island. The integrals in this case are considerably simplified by the use of polar coordinates and the symmetry of the problem. Let us consider first the special case $R(0, 0, 0)$, the mean-square pressure at the wall. Equation (6) after integration yields

$$\overline{P^{*2}} = \overline{P_o^{*2}} - 26.8 Q B - 23.5 Q^2 B, \quad (49)$$

where $Q = (\rho U_\infty / \rho_o C_s) Y_n^* (\infty)$. However, we note from direct integration of Eq. (44) that

$$\overline{P^{*2}} = 25 B, \quad (50)$$

which we may use to eliminate B from Eq. (49). The result is the following final estimate for the general effect of the compliant coating:

$$\overline{P^{*2}} = \frac{\overline{P_o^{*2}}}{1 + 1.07 Q + 0.94 Q^2} \quad \begin{array}{l} \text{(Thick} \\ \text{Coating)} \end{array} \quad (51)$$

The numerical constants 1.07 and 0.94 are not particularly accurate and a rounded value of unity would probably suffice for both. For example, by attempting slightly different curve-fits to Fig. 7, both constants can be varied as much as twenty per cent.

Since the factor Q is negative for subcritical speeds from Table 2, Eq. (51) indicates that the coating effect is mixed in character. The mean wall pressure fluctuation is actually increased at low speeds and is decreased only for near-critical speeds. If we assume an average value of 1.5 for the convection speed ratio U_∞ / U_c , Eq. (51) may be plotted versus the speed ratio U_∞ / C_s for a given coating. Further let us assume that the coating has a specific gravity of 1.0 and Poisson's ratio of 0.5. Figure 11 shows the effect of the coating on the mean square wall pressure in this case for both plane stress and plane strain admittances from Table 2.

Figure 11, while representing the central result of this study, is very probably only a qualitative estimate, because of the many approximations encountered en route to its derivation. However, this analysis clearly predicts qualitatively that the coating increases the wall pressure slightly at low speeds and causes a dramatic decrease at higher speeds. However, the dash-dot vertical line in Fig. 11 shows the prediction of Ref. 26 that the coating suffers

a static divergence at $U_\infty = C_s$. The accuracy of this static instability prediction is not known, but it appears probable that it will be difficult to achieve the hoped for reduction in flow noise because of the coating's own instability.

Equation (51) and Fig. 11 are valid for an asymptotically thick coating. A reduction in thickness would merely modify the constants in Eq. (51). That is, in general,

$$\overline{P^{*2}} = \frac{\overline{P_o^{*2}}}{1 + m_1 Q + m_2 Q^2}, \quad (52)$$

where m_1 and m_2 are functions of thickness ratio (h/δ), with asymptotic values of 1.07 and 0.94, respectively. Figure 12 shows calculated values of these constants as a function of thickness. It is seen that a thin coating is surprisingly effective and that there is no point in increasing the coating thickness beyond $h = \delta$.

• It is necessary to check these calculations by computing the power spectrum in the presence of the coating, since it was assumed in Eq. (44) that ϕ was identical in shape to the rigid wall spectrum of Fig. 7 and merely scaled up or down in magnitude. To check this point, we must calculate the autocorrelation $R(0,0,t_o)$ from Eq. (6) and take its inverse Fourier transform. It is sufficient to consider only the excess of R over the rigid wall value R_o , which we may put in normalized form by defining the following factor f :

$$f(t_o^*) = \frac{R(0,0,t_o^*) - R_o(0,0,t_o^*)}{R(0,0,0) - R_o(0,0,0)}. \quad (53)$$

Some numerical results for $f(t_o^*)$ are compared in Table 3 with the exponential approximation $e^{-12 t_o^*}$.

Table 3

NORMALIZED EXCESS AUTOCORRELATION FOR A THICK COATING

t_o^*	$f(t_o^*)$	$e^{-12 t_o^*}$
0.0	1.000	1.000
0.1	0.296	0.301
0.2	0.086	0.091
0.3	0.034	0.027

It is seen that the exponential approximation is sufficiently accurate to use in estimating the shift in the power spectrum, which is easily evaluated for an exponential:

$$\Delta \phi \sim \int_0^{\infty} e^{-12 t_o^*} \cos (\omega^* t_o^*) dt_o^* \sim \frac{1}{1 + (\omega^*/12)^2} \quad (54)$$

This additional power spectrum should be added to ϕ_o to account for the presence of the coating. Equation (54) indicates that the corrected spectrum should be very similar in shape to the rigid wall spectrum, thus verifying the assumption made by Eq. (44).

Equation (54) predicts that the compliant coating has the effect of essentially raising or lowering the entire power spectrum curve until the area under it - the mean-square pressure - equals the value predicted by Eq. (52). However, at present, it would be nearly impossible to verify this effect experimentally with the transducers now available. For, from Figs. 9 and 10, we see that the time-averaged effect of a compliant coating is confined to a very narrow area about the point being studied, with a diameter roughly equal to one-tenth of the boundary layer thickness. Thus, a transducer capable of measuring such localized effects would need a shank whose diameter was another order of magnitude smaller, say, one-hundredth of the boundary layer thickness. Since the smallest available transducer has a shank diameter of approximately 0.1 inch, it is seen that accurate spectrum measurements would require a boundary layer thickness of ten inches or greater. Even then, the coating dynamics would surely be modified by the presence of the relatively rigid shank protruding through its thickness.

PRESSURE ATTENUATION BENEATH A COMPLIANT COATING

Since the previous analysis does not predict any clearly attainable noise reduction at the upper surface, it is natural to look elsewhere for a practical solution to the problem. One possibility is the expectation that the pressure fluctuations at the "upper" or boundary layer surface might be attenuated through the coating thickness and be much smaller at the "lower" or bonded surface.

Returning to the previous traveling wave study, we may define an attenuation factor "F" as a lower-to-upper pressure ratio for any given traveling wave of the form of Eq. (7):

$$F = \frac{\sigma_{22}(-h)}{\sigma_{22}(0)} \quad (55)$$

The dimensionless factor F should depend upon frequency (αh), speed ratio (U_c/C_s), Poisson's ratio (μ), the type of bond (shearless or bonded), and the geometry (plane stress or plane strain).

If we confine our attention to the bonded coating in a condition of plane stress, the attenuation factor F may be written in terms of the quantities r_1 , C_1 , and T_1 from Eqs. (11) and (18), as follows:

$$F = \frac{r_1 r_2 (U_c/C_s)^2 [2 C_1 - (1 + r_2^2) C_2]}{C_1 C_2 (T_2 - r_1 r_2 T_1) [2 (1 + r_2^2) A_1 + 4 r_1 r_2 A_3]} \quad (56)$$

where A_1 and A_3 are the constants given by Eq. (19). At very low frequencies, F is unity, while at very high frequencies F is inversely proportional to C_2 , that is, exponentially decreasing. Figure 13 shows the frequency variation of F for Poisson's ratio equal to one-half and for various subcritical speed ratios. It is seen that the pressure attenuation through the thickness is much greater at low speeds.

With the frequency distribution of F known, the total attenuating effect of a bonded coating is determined by simple integration over the frequency range. If $\phi(\omega)$ is the power spectrum of pressure at the upper surface, the mean-square pressure at the lower surface is given by

$$\overline{P^2(-h)} = 2 \int_0^\infty F^2 \phi(\omega) d\omega \quad (57)$$

Since F is a function of (αh) and ϕ is a function of ($\alpha \delta$), the integral in Eq. (57) depends upon the thickness ratio (h/δ). If we take ϕ to be given by Eq. (44), and if F is given by Eq. (56), then Eq. (57) may be evaluated numerically. The results are shown in Fig. 14, indicating the reduction in mean-square pressure beneath the surface as a function of speed ratio (U_c/C_s) for various coating thicknesses. It is seen that even a rather thin coating will cause a substantial mean-pressure reduction through its thickness, particularly at low speeds. One also notes that a very thick coating will give a dramatic decrease in lower surface pressure level.

LIST OF REFERENCES

- ¹ M.O. Kramer, "Boundary Layer Stabilization by Distributed Damping," Journal of Aeronautical Sciences, vol. 24, 1957, p. 459.
- ² M.O. Kramer, "Readers Forum," Journal of Aero/Space Sciences, vol. 27, 1960, p. 68.
- ³ M.O. Kramer, "Boundary Layer Stabilization by Distributed Damping," Journal American Society Naval Engineers, vol. 72, February 1960, p. 25.
- ⁴ F.W. Boggs and N. Tokita, "A Theory of Stability of Laminar Flow Along Compliant Plates," Third Symposium on Naval Hydrodynamics, Schereningen (The Hague), Netherlands, September 1960.
- ⁵ T.B. Benjamin, "Effects of a Flexible Boundary on Hydrodynamic Stability," Journal of Fluid Mechanics, vol. 9, 1960, p. 513.
- ⁶ T.B. Benjamin, "The Threefold Classification of Unstable Disturbances in Flows over Flexible Surfaces," Journal of Fluid Mechanics, vol. 16, p. 436.
- ⁷ T. Nonweiler, Qualitative Solutions of the Stability Equation for a Boundary Layer in Contact with Various Forms of Flexible Surfaces, British A.R.C. Report No. 22,670, 1961.
- ⁸ J.H. Linebarger, "On the Stability of a Laminar Boundary Layer over a Flexible Surface in a Compressible Fluid," S.M. Thesis, Department of Aeronautics and Astronautics, Massachusetts Institute of Technology, 1961.
- ⁹ M.T. Landahl, "On the Stability of a Laminar, Incompressible Boundary Layer over a Flexible Surface," Journal of Fluid Mechanics, vol. 13, 1962, p. 609.
- ¹⁰ F.D. Hains, Comparison of the Stability of Poiseuille Flow and the Blasius Profile for Flexible Walls, Boeing Scientific Research Laboratories, Flight Sciences Laboratory Report No. 75, 1963.
- ¹¹ R.E. Kaplan, "The Stability of Laminar Incompressible Boundary Layers in the Presence of Compliant Boundaries," Sc. D. Thesis, Massachusetts Institute of Technology, Department of Aeronautics and Astronautics, 1964.
- ¹² W.A. VonWinkle, "An Evaluation of a Boundary Layer Stabilization Coating," USL Technical Memorandum No. 922-111-61, 1961.
- ¹³ F.W. Boggs and H.R. Frey, The Effect of a Lamiflo Coating on a Small Planing Hull Having Zero Deadrise, U.S. Rubber Company Report, June 1961.

- 14 J. Laufer and L. Maestrello, "The Turbulent Boundary Layer over a Flexible Surface," The Boeing Company, Document No. D6-9708, 1963.
- 15 J.E. Ffowcs Williams and R.H. Lyon, The Sound Radiated from Turbulent Flows near Flexible Boundaries, BBN Report No. 1054, 1963.
- 16 J.E. Ffowcs Williams, Reynolds Stress near a Flexible Surface Responding to Unsteady Air Flow, Bolt Beranek and Newman Inc., Report No. 1138, Cambridge, Massachusetts, June 1964.
- 17 G.M. Corcos, "The Structure of the Turbulent Pressure Field in Boundary-Layer Flows," Journal of Fluid Mechanics, vol. 18, 1964, p. 353.
- 18 H.P. Bakewell, G.F. Carey, J.J. Libuha, H.H. Schloemer, and W.A. VonWinkle, Wall Pressure Correlations in Turbulent Pipe Flow, USL Report No. 559, 20 August 1962.
- 19 W.W. Willmarth and C.E. Wooldridge, "Measurements of the Fluctuating Pressure at the Wall Beneath a Thick Turbulent Boundary Layer," Journal of Fluid Mechanics, vol. 14, p. 187.
- 20 S. Gardner, On Surface Pressure Fluctuations Produced by Boundary Layer Turbulence, Technical Research Group Inc., Report No. TRG-142-TN-63-5, October 1963.
- 21 S. Gardner, "On Surface Pressure Fluctuations Produced by Boundary Layer Turbulence," Acustica, vol. 16, No. 2, 1965/66, p. 67.
- 22 F.M. White, A Unified Theory of Turbulent Wall Pressure Fluctuations, USL Report No. 629, 1 December 1964.
- 23 H.H. Schloemer, Effect of Pressure Gradients on Turbulent Boundary-Layer Wall-Pressure Fluctuations, USL Report No. 747, 1 July 1966.
- 24 R.H. Kraichnan, "Pressure Fluctuations in Turbulent Flow over a Flat Plate," Journal of the Acoustical Society of America, vol. 28, No. 3, May 1956, p. 378.
- 25 N. Tokita and F.W. Boggs, Theoretical Study of Compliant Coatings to Achieve Drag Reduction in Underwater Vehicles, U.S. Rubber Company, Final Report, U.S. Navy Contract Nonr 3120 (00), 16 May 1962.
- 26 F.W. Boggs and N. Tokita, Hydroelastic Behavior of Compliant Coatings, U.S. Rubber Company Report, Navy Contract Nbw-60-0676-C, 19 June 1963.

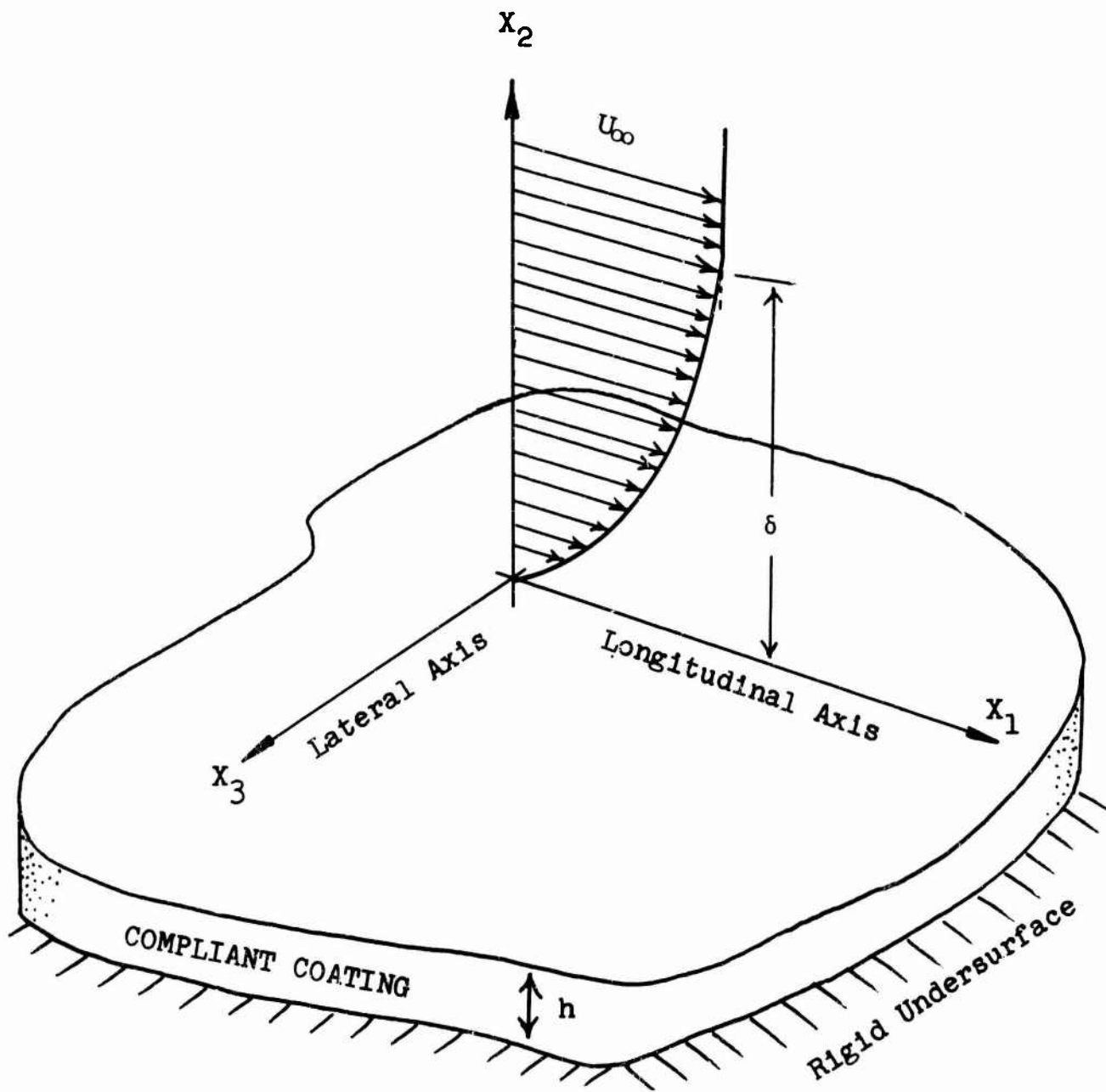


Fig. 1 - Schematic of the Flow Geometry

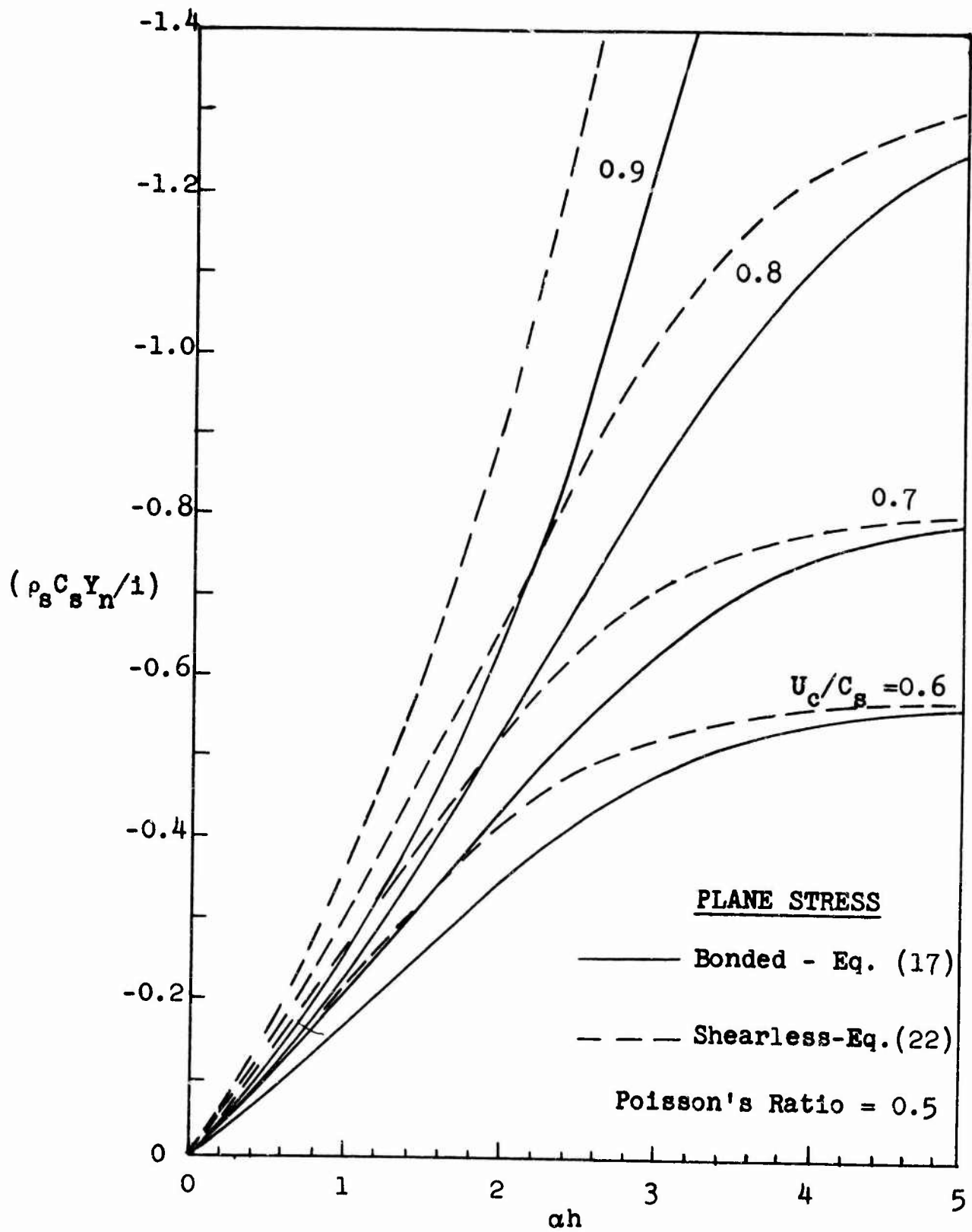


Fig. 2 - Comparison of Normal Admittance Y_n for the Bonded and Shearless Coating

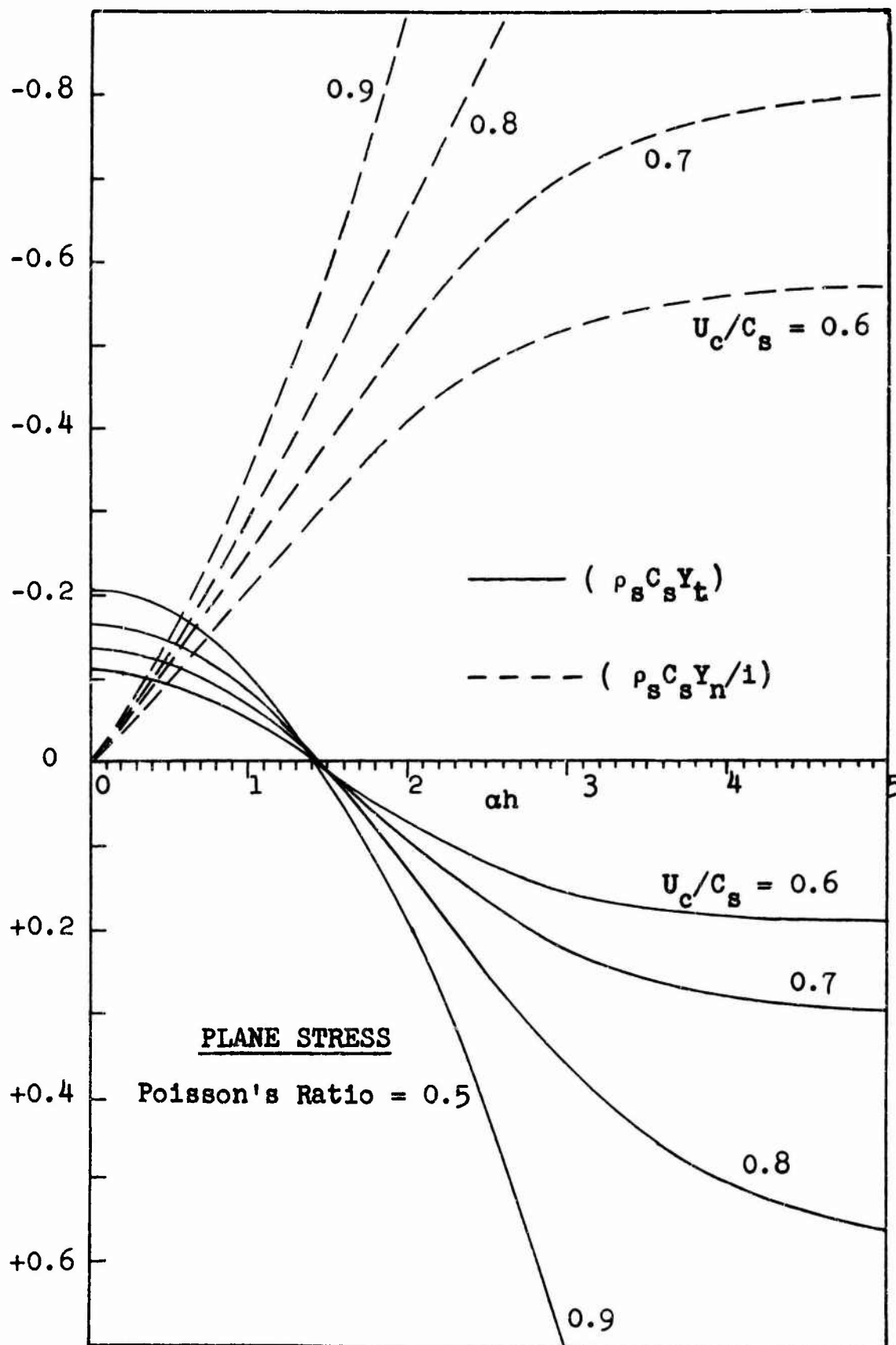


Fig. 3 - Comparison of Tangential Admittance Y_t and Normal Admittance Y_n for a Shearless Coating

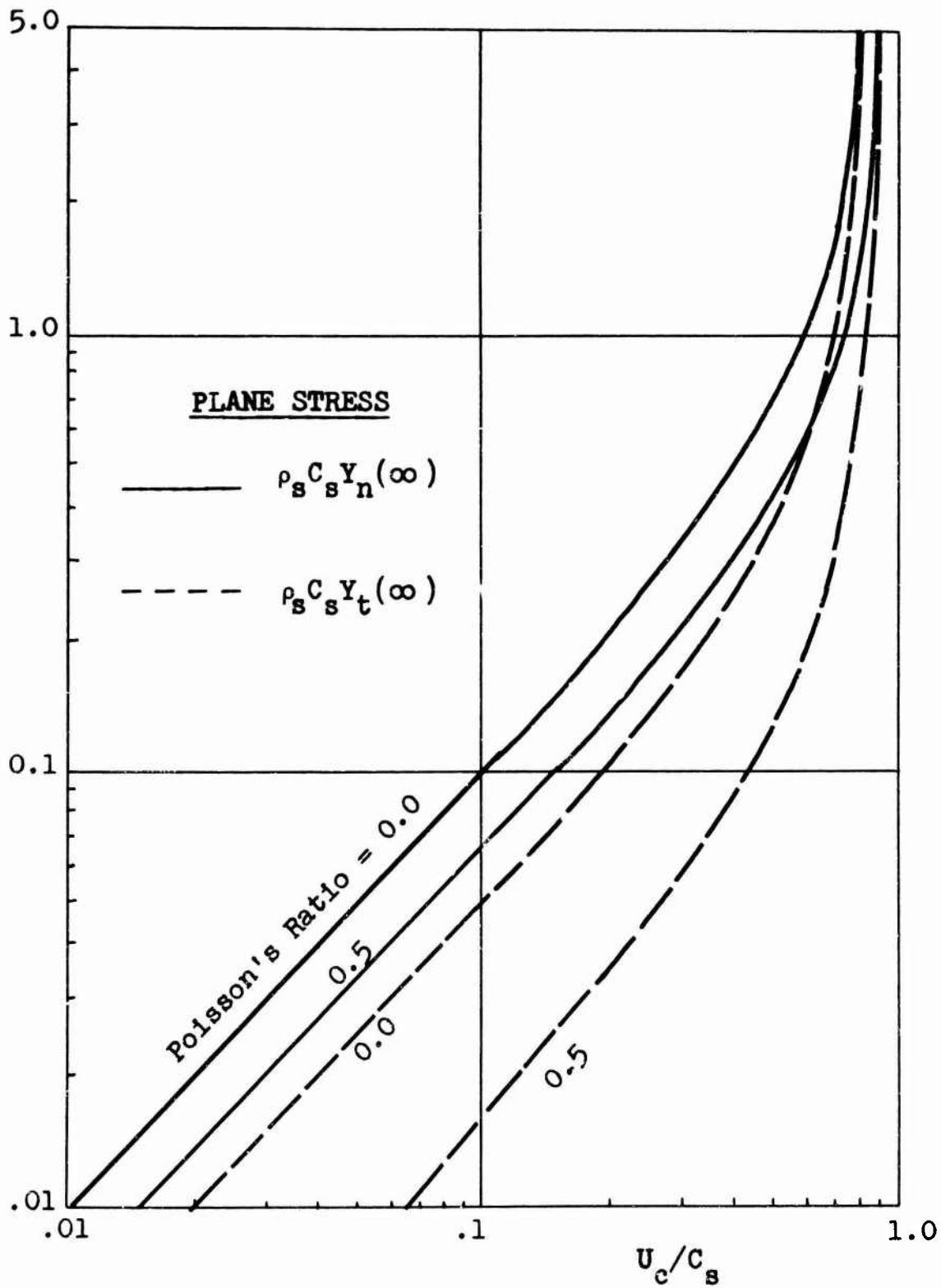


Fig. 4 - Magnitude of the Asymptotic Plane Stress Admittances as a Function of Speed Ratio

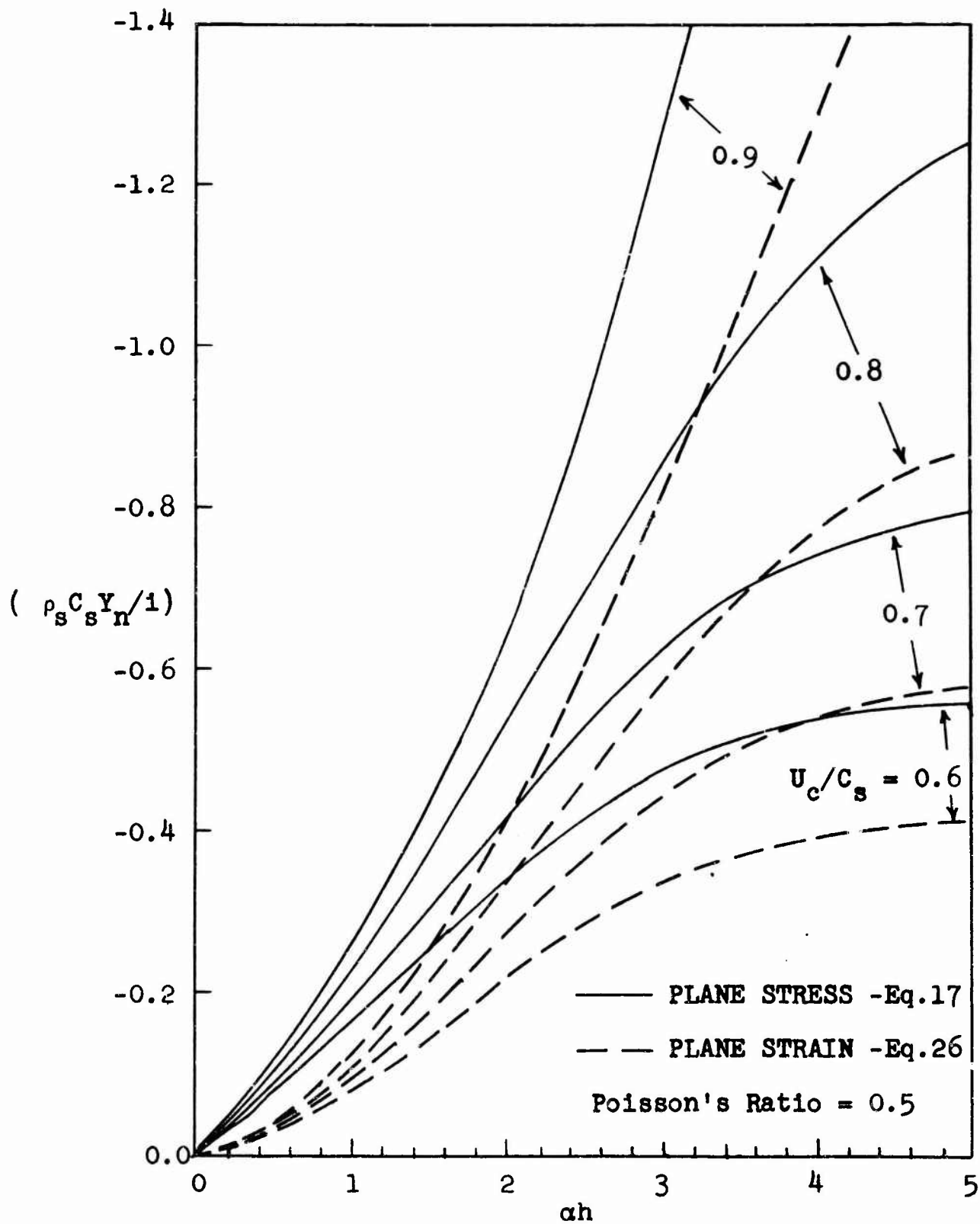


Fig. 5 - Comparison of the Normal Admittance Y_n for Plane Stress versus Plane Strain

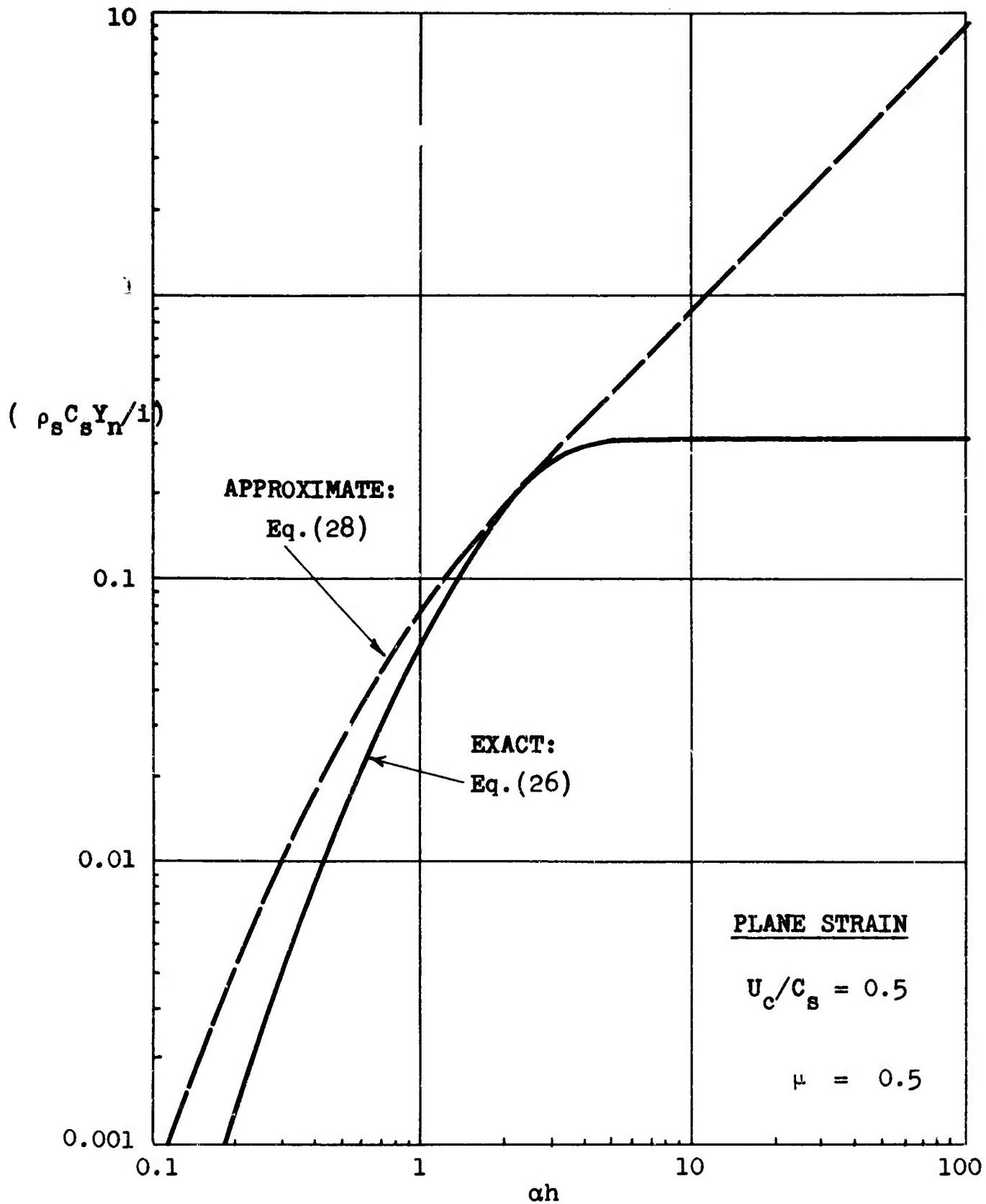


Fig. 6 - Comparison of Exact and Approximate Normal Admittances Y_n for Plane Strain

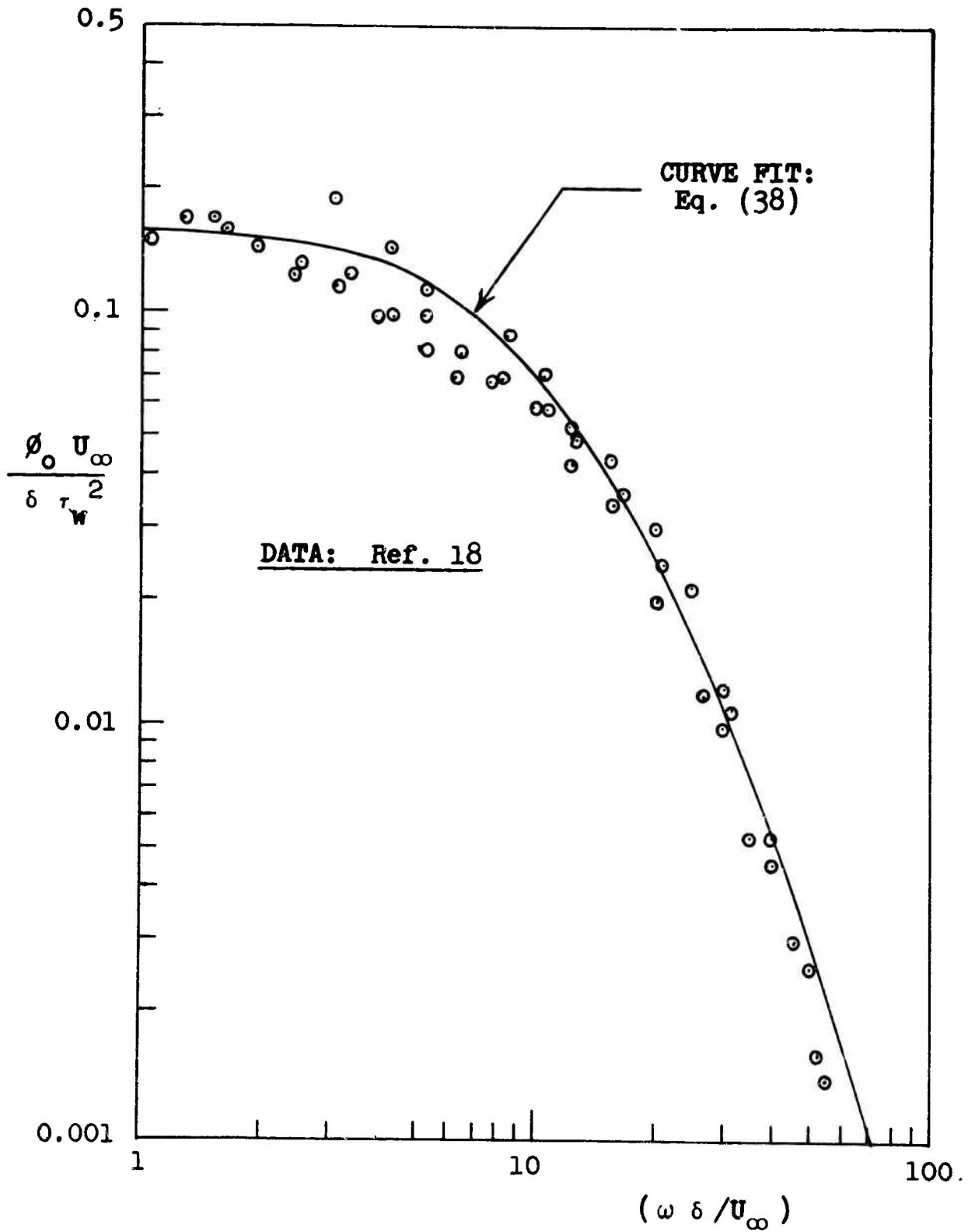


Fig. 7 - Experimental Data for the Power Spectrum of Rigid Wall Turbulent Pressure

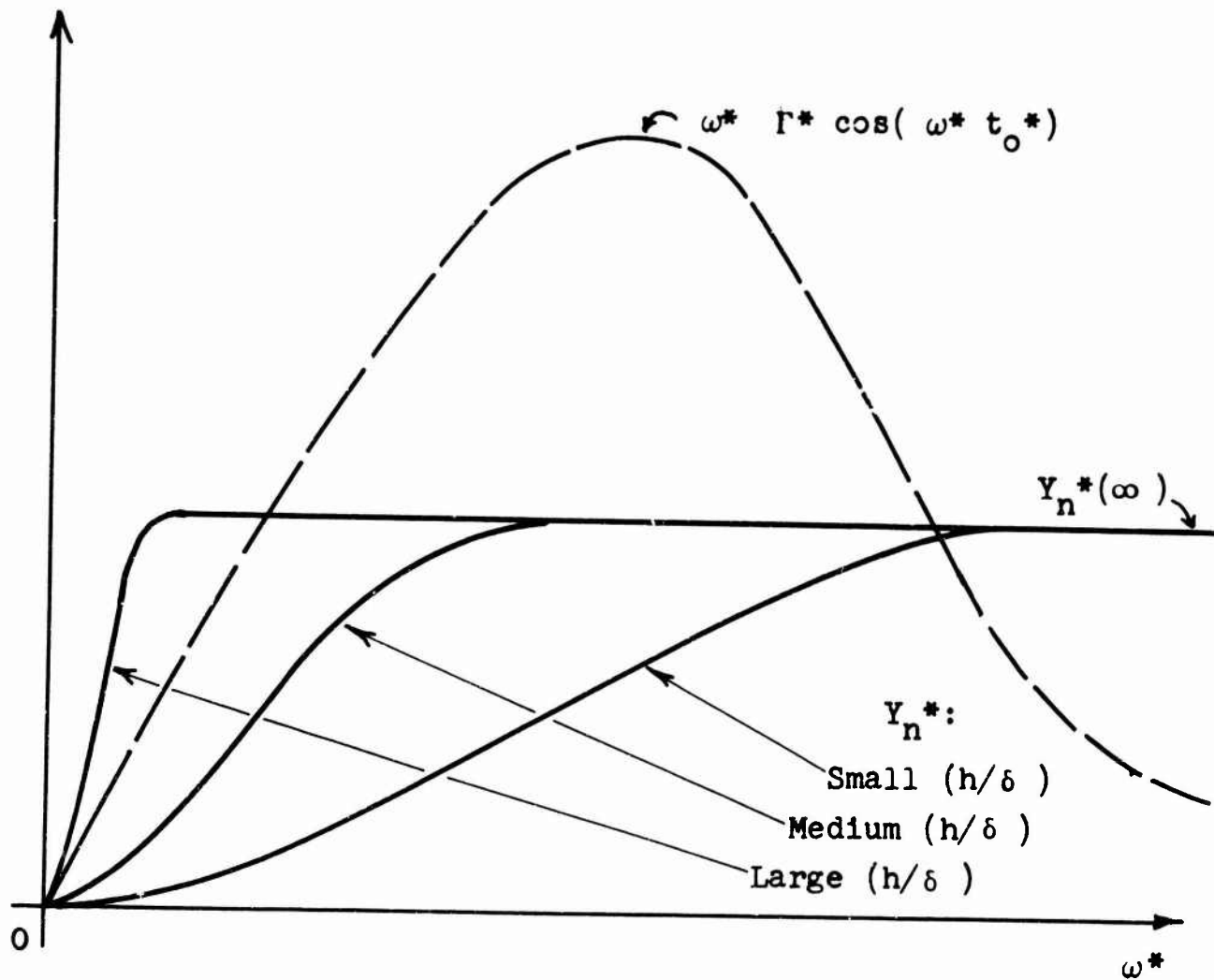


Fig. 8 - Illustration of the Effect of Thickness Ratio (h/δ) on the Integrand of Eq. (40)

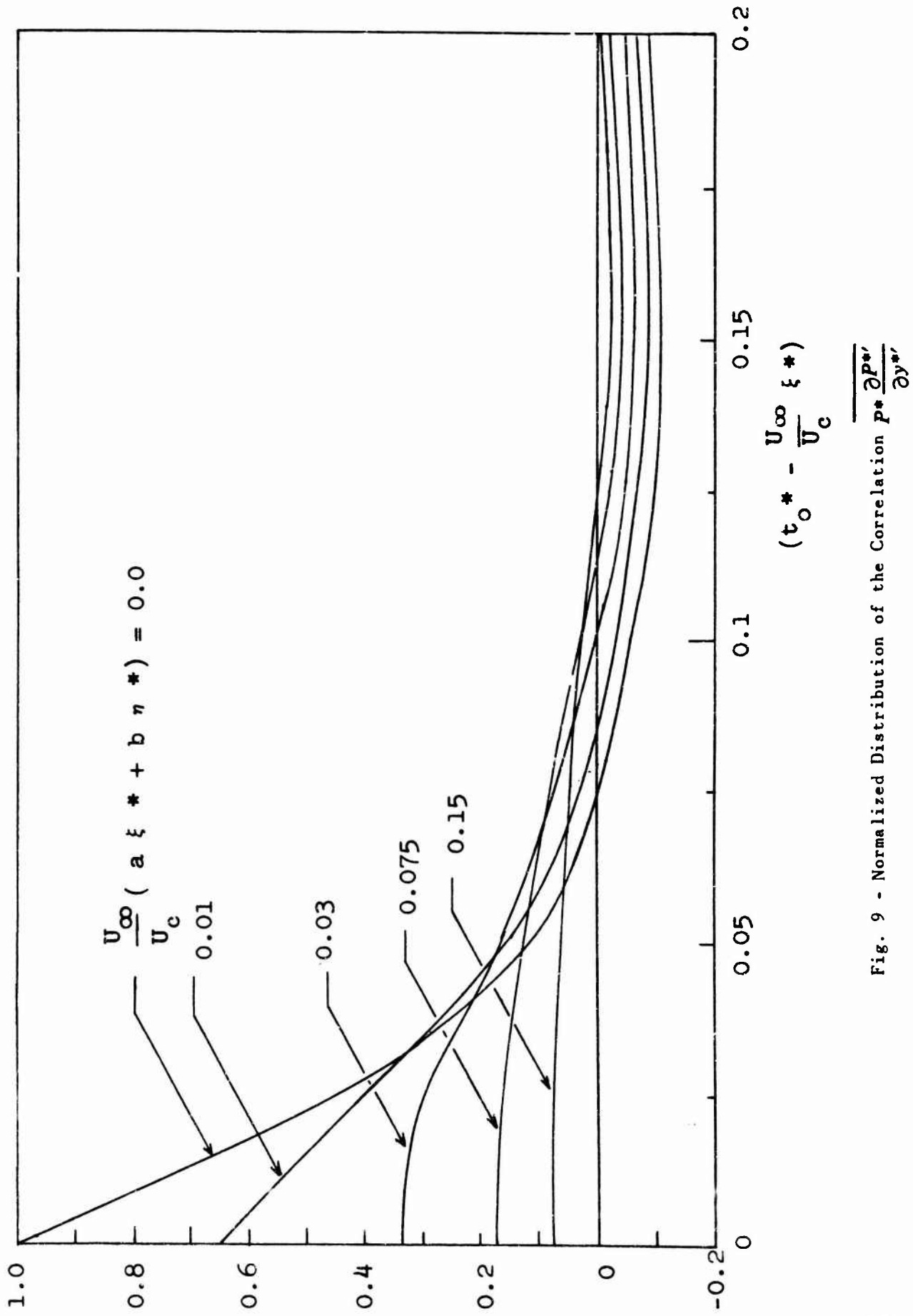


Fig. 9 - Normalized Distribution of the Correlation $P^* \frac{\partial P^*}{\partial y^*}$

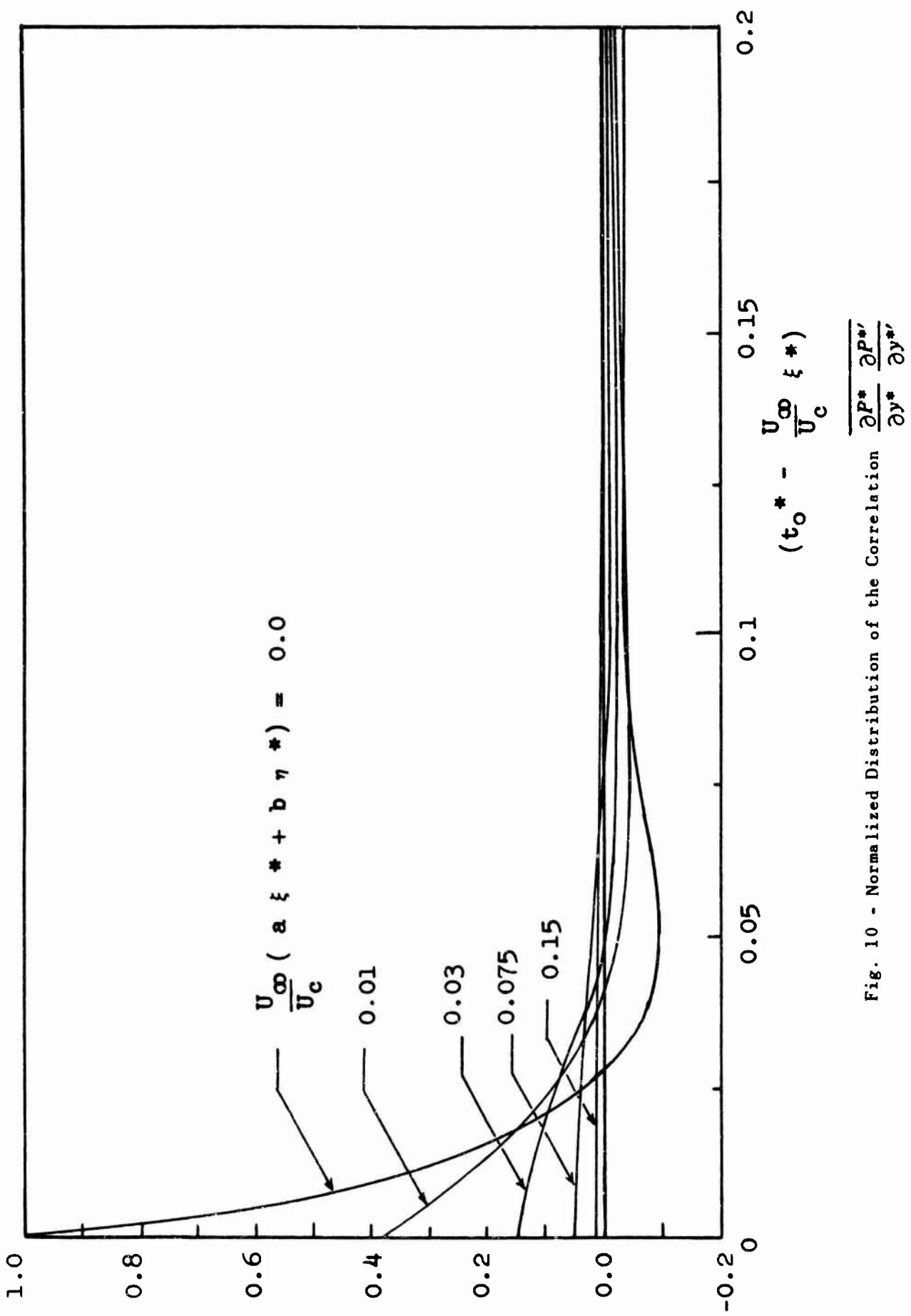


Fig. 10 - Normalized Distribution of the Correlation $\frac{\partial P^*}{\partial y^*} \frac{\partial P^*}{\partial y^*}$

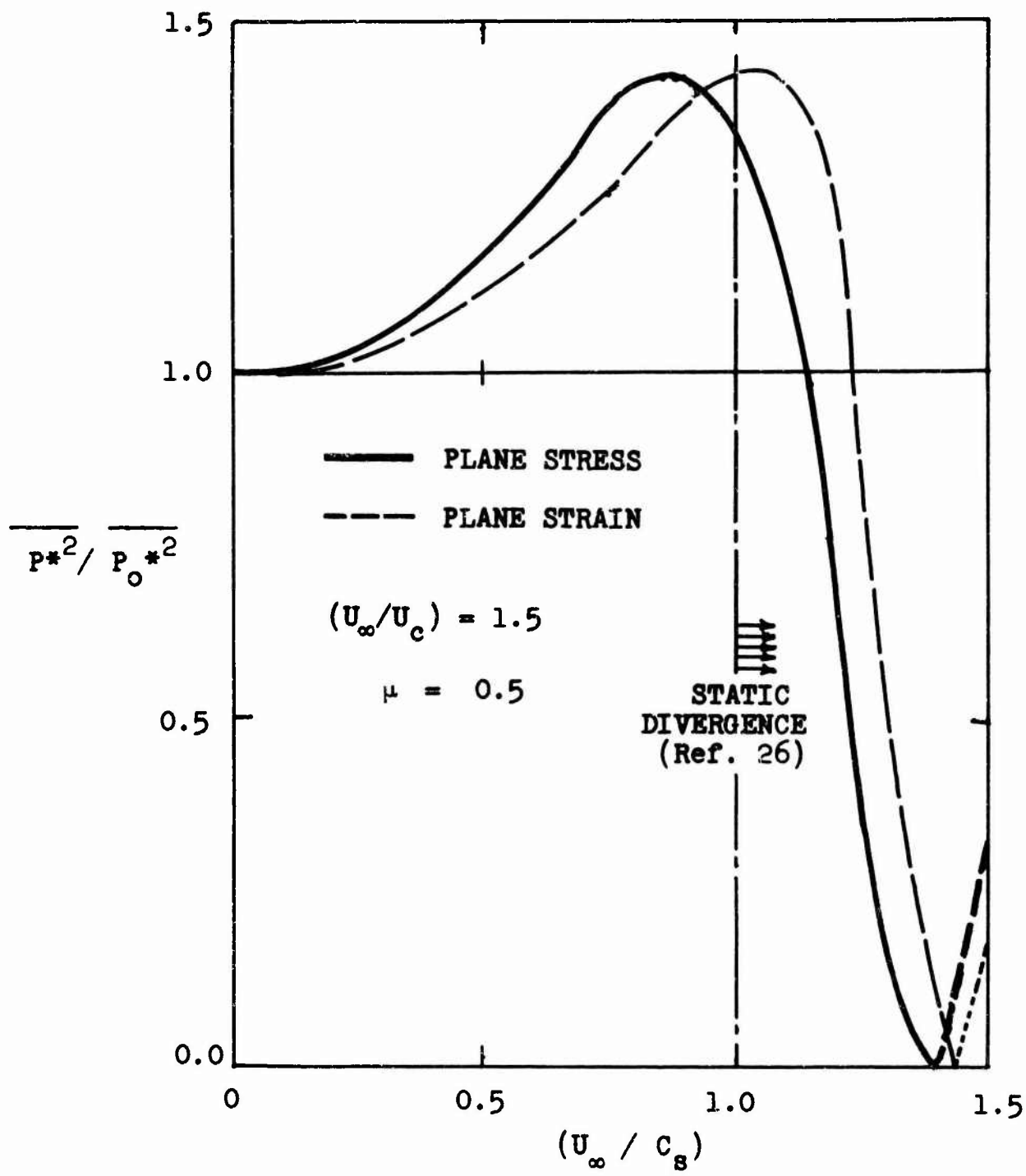


Fig. 11 - Final Estimation of the Effect of a Compliant Coating on the Wall Pressure

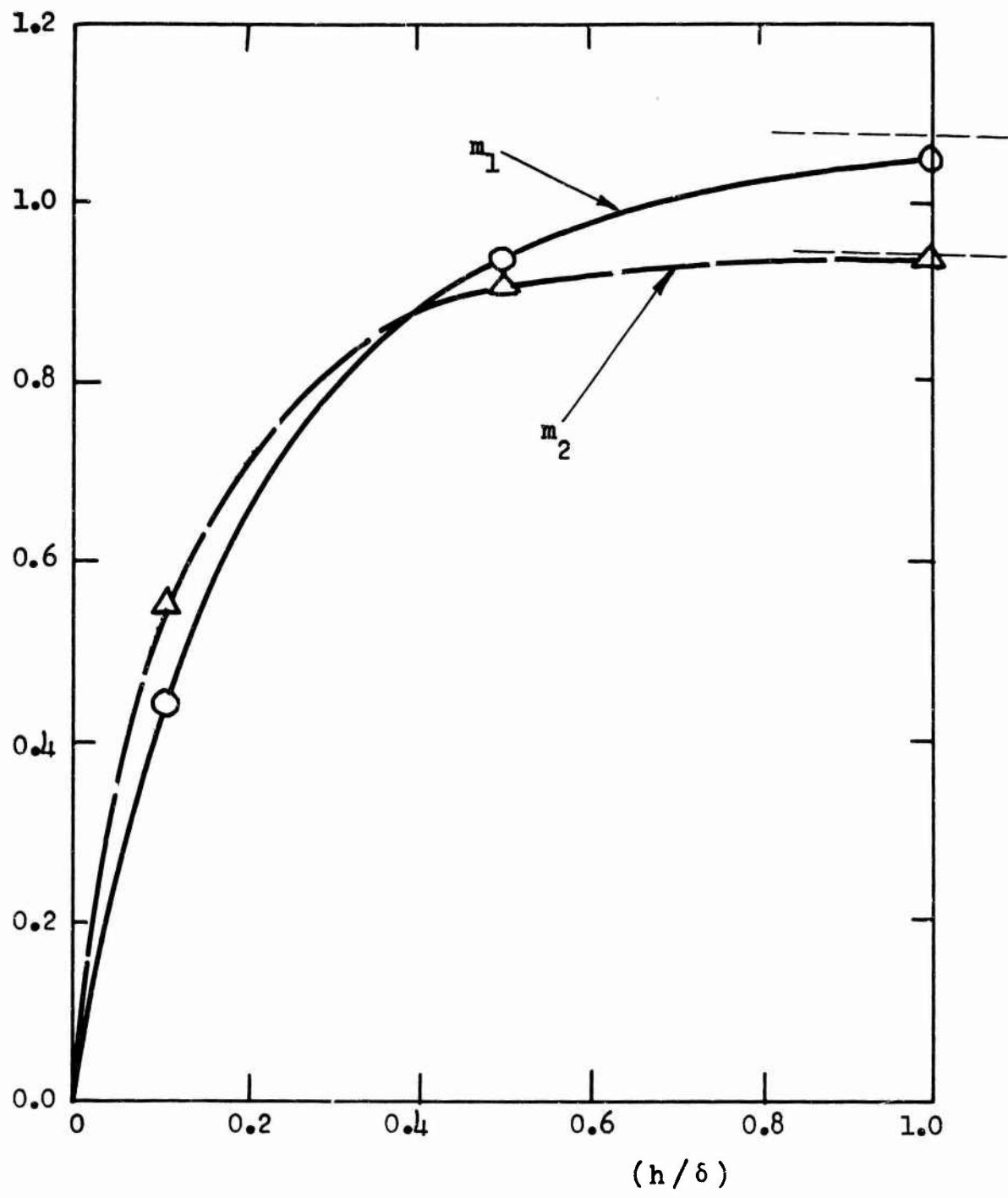


Fig. 12 - Effect of Coating Thickness on the Attenuation Constants in Eq. (52)

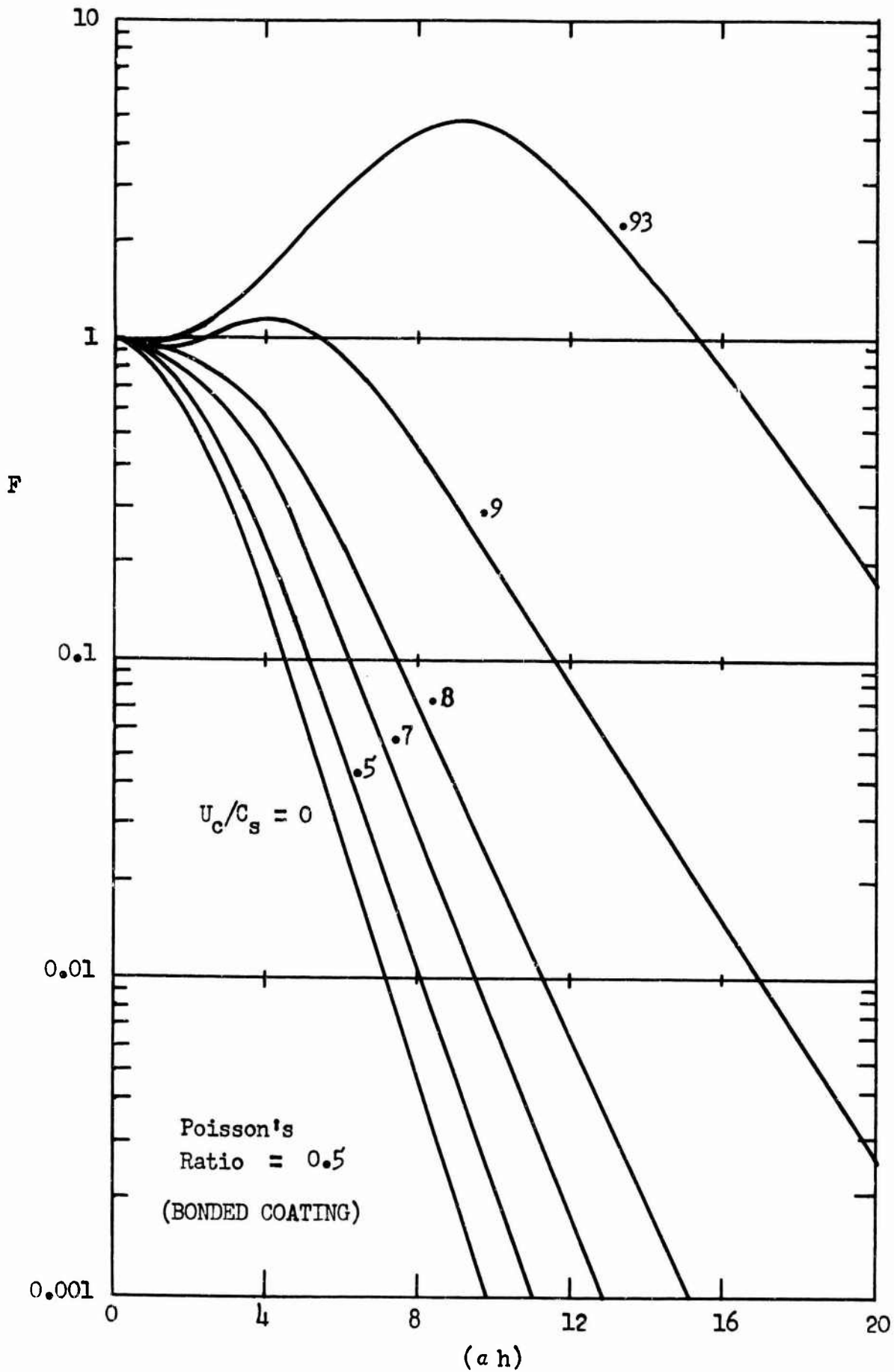


Fig. 13 - Pressure Attenuation Factor F as a Function of Frequency and Speed

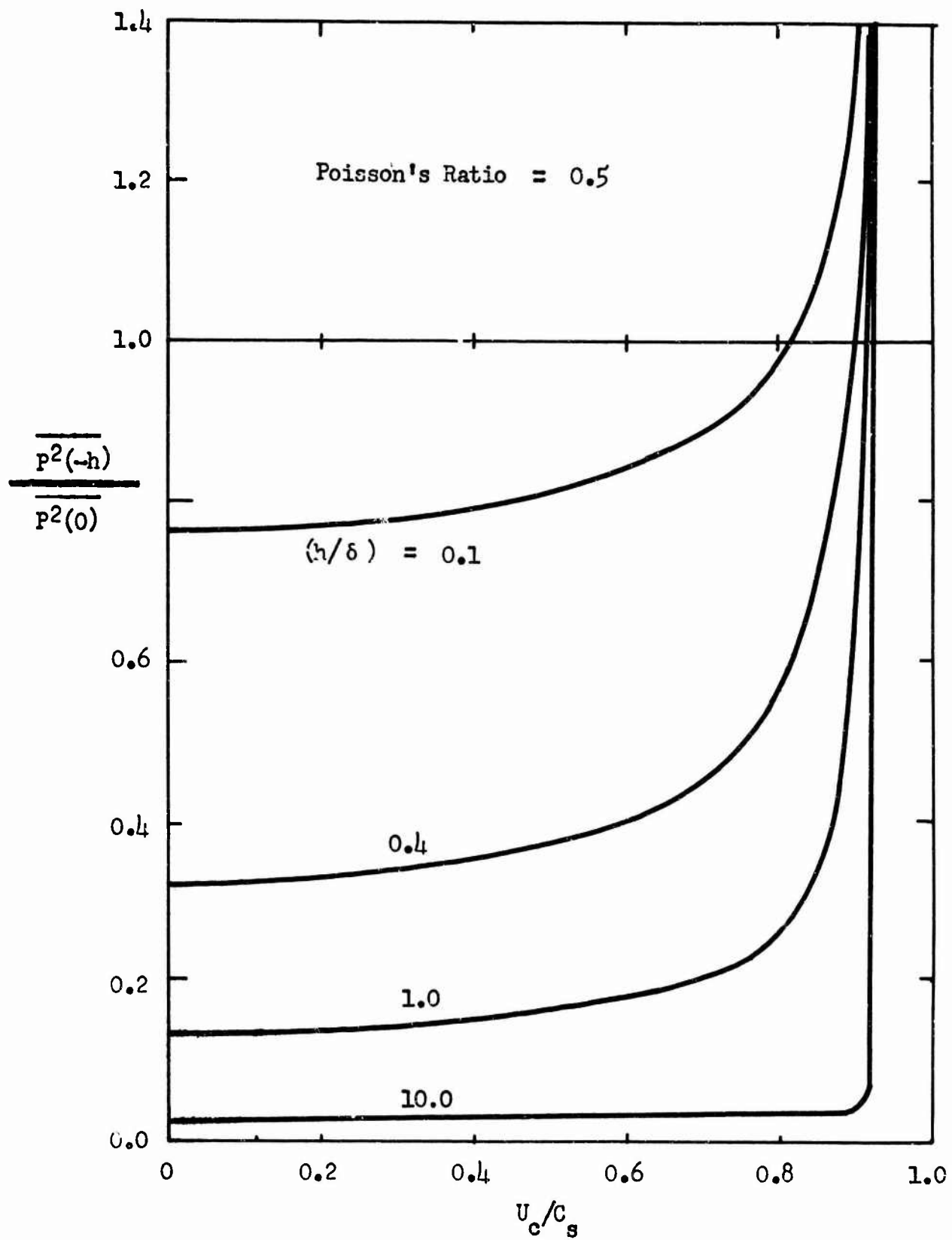


Fig. 14 - Reduction of Undersurface Pressure Level as a Function of Speed Ratio and Thickness Ratio

UNCLASSIFIED

Security Classification

DOCUMENT CONTROL DATA - R&D

(Security classification of title, body of abstract and indexing annotation must be entered when the overall report is classified)

1. ORIGINATING ACTIVITY (Corporate author) U. S. Navy Underwater Sound Laboratory Fort Trumbull, New London, Connecticut		2a. REPORT SECURITY CLASSIFICATION UNCLASSIFIED	
		2b. GROUP	
3. REPORT TITLE A THEORETICAL ESTIMATE OF TURBULENT WALL PRESSURE FLUCTUATIONS ON A COMPLIANT BOUNDARY			
4. DESCRIPTIVE NOTES (Type of report and inclusive dates) Research Report			
5. AUTHOR(S) (Last name, first name, initial) White, Frank M. Quaglieri, Robert E.			
6. REPORT DATE 23 November, 1966	7a. TOTAL NO. OF PAGES 45	7b. NO. OF REFS 26	
8a. CONTRACT OR GRANT NO. 70024-44754	8a. ORIGINATOR'S REPORT NUMBER(S) 767		
A. PROJECT NO. SF 113 11 08-1356	8b. OTHER REPORT NO(S) (Any other numbers that may be assigned this report)		
c.			
d.			
10. AVAILABILITY/LIMITATION NOTICES Distribution of this document is unlimited			
11. SUPPLEMENTARY NOTES		12. SPONSORING MILITARY ACTIVITY U. S. Navy	
13. ABSTRACT A theoretical estimate is attempted for the effect of a compliant coating on turbulent boundary layer wall pressure fluctuations. The basic derivation shows that the problem reduces to one of finding the distribution in the wall plane of two correlations involving the wall pressure and its normal derivative. Exact expressions are derived for two-dimensional traveling wave pressure/velocity admittance of an isotropic elastic coating. These admittances are combined with some reasonable assumptions about the form of the pressure cross spectral density to yield approximate expressions for the two desired pressure/derivative correlations. Finally, two surface integrals of these correlations result in the wall pressure function in the presence of the compliant boundary. The calculations indicate that the compliant wall increases the mean square wall pressure at low speeds and decreases the pressure fluctuations at high speeds. Unfortunately, the reduction at high speeds probably cannot be achieved in practice because of the related mechanical problem of static divergence of the coating.			

14 KEY WORDS	LINK A		LINK B		LINK C	
	ROLE	WT	ROLE	WT	ROLE	WT
Flow noise Turbulent flow Boundary layer theory Wall pressure fluctuations Turbulent boundary layer						

INSTRUCTIONS

1. ORIGINATING ACTIVITY: Enter the name and address of the contractor, subcontractor, grantee, Department of Defense activity or other organization (corporate author) issuing the report.

2a. REPORT SECURITY CLASSIFICATION: Enter the overall security classification of the report. Indicate whether "Restricted Data" is included. Marking is to be in accordance with appropriate security regulations.

2b. GROUP: Automatic downgrading is specified in DoD Directive 5200.10 and Armed Forces Industrial Manual. Enter the group number. Also, when applicable, show that optional markings have been used for Group 3 and Group 4 as authorized.

3. REPORT TITLE: Enter the complete report title in all capital letters. Titles in all cases should be unclassified. If a meaningful title cannot be selected without classification, show title classification in all capitals in parenthesis immediately following the title.

4. DESCRIPTIVE NOTES: If appropriate, enter the type of report, e.g., interim, progress, summary, annual, or final. Give the inclusive dates when a specific reporting period is covered.

5. AUTHOR(S): Enter the name(s) of author(s) as shown on or in the report. Enter last name, first name, middle initial. If military, show rank and branch of service. The name of the principal author is an absolute minimum requirement.

6. REPORT DATE: Enter the date of the report as day, month, year, or month, year. If more than one date appears on the report, use date of publication.

7a. TOTAL NUMBER OF PAGES: The total page count should follow normal pagination procedures, i.e., enter the number of pages containing information.

7b. NUMBER OF REFERENCES: Enter the total number of references cited in the report.

8a. CONTRACT OR GRANT NUMBER: If appropriate, enter the applicable number of the contract or grant under which the report was written.

8b, 8c, & 8d. PROJECT NUMBER: Enter the appropriate military department identification, such as project number, subproject number, system numbers, task number, etc.

9a. ORIGINATOR'S REPORT NUMBER(S): Enter the official report number by which the document will be identified and controlled by the originating activity. This number must be unique to this report.

9b. OTHER REPORT NUMBER(S): If the report has been assigned any other report numbers (either by the originator or by the sponsor), also enter this number(s).

10. AVAILABILITY/LIMITATION NOTICES: Enter any limitations on further dissemination of the report, other than those

imposed by security classification, using standard statements such as:

- (1) "Qualified requesters may obtain copies of this report from DDC."
- (2) "Foreign announcement and dissemination of this report by DDC is not authorized."
- (3) "U. S. Government agencies may obtain copies of this report directly from DDC. Other qualified DDC users shall request through _____."
- (4) "U. S. military agencies may obtain copies of this report directly from DDC. Other qualified users shall request through _____."
- (5) "All distribution of this report is controlled. Qualified DDC users shall request through _____."

If the report has been furnished to the Office of Technical Services, Department of Commerce, for sale to the public, indicate this fact and enter the price, if known.

11. SUPPLEMENTARY NOTES: Use for additional explanatory notes.

12. SPONSORING MILITARY ACTIVITY: Enter the name of the departmental project office or laboratory sponsoring (paying for) the research and development. Include address.

13. ABSTRACT: Enter an abstract giving a brief and factual summary of the document indicative of the report, even though it may also appear elsewhere in the body of the technical report. If additional space is required, a continuation sheet shall be attached.

It is highly desirable that the abstract of classified reports be unclassified. Each paragraph of the abstract shall end with an indication of the military security classification of the information in the paragraph, represented as (TS), (S), (C), or (U).

There is no limitation on the length of the abstract. However, the suggested length is from 150 to 225 words.

14. KEY WORDS: Key words are technically meaningful terms or short phrases that characterize a report and may be used as index entries for cataloging the report. Key words must be selected so that no security classification is required. Identifiers, such as equipment model designation, trade name, military project code name, geographic location, may be used as key words but will be followed by an indication of technical content. The assignment of links, roles, and weights is optional.